Methods. Author manuscript; available in PMC 2020 March 27.

Published in final edited form as:
Methods. 2019 July 22; 174: 27–41. doi:10.1016/j.ymeth.2019.07.019.

Strategies to maximize performance in STimulated Emission Depletion (STED) nanoscopy of biological specimens

Wiebke Jahr, **Philipp Velicky**, **Johann Georg Danzl**[1]
Institute of Science and Technology, Austria, Am Campus 1, 3400 Klosterneuburg, Austria

Abstract

Super-resolution fluorescence microscopy has become an important catalyst for discovery in the life sciences. In STimulated Emission Depletion (STED) microscopy, a pattern of light drives fluorophores from a signal-emitting on-state to a non-signalling off-state. Only emitters residing in a sub-diffraction volume around an intensity minimum are allowed to fluoresce, rendering them distinguishable from the nearby, but dark fluorophores. STED routinely achieves resolution in the few tens of nanometers range in biological samples and is suitable for live imaging. Here, we review the working principle of STED and provide general guidelines for successful STED imaging. The strive for ever higher resolution comes at the cost of increased light burden. We discuss techniques to reduce light exposure and mitigate its detrimental effects on the specimen. These include specialized illumination strategies as well as protecting fluorophores from photobleaching mediated by high-intensity STED light. This opens up the prospect of volumetric imaging in cells and tissues with diffraction-unlimited resolution in all three spatial dimensions in living samples.

Keywords

Fluorescence Microscopy; Optical Imaging; Super-Resolution Microscopy; Nanoscopy; Stimulated Emission Depletion Microscopy; STED, Protected STED; Live Imaging; Photodamage

1 Introduction

Light microscopy is an extremely valuable tool for the life sciences. Its broad usefulness is underscored by the following features: (1) Sample preparation is often straightforward. (2) Light microscopy is uniquely suited to attain molecular contrast and, in multicolour measurements, to visualize mutual spatial arrangements. (3) Fluorescence microscopy boasts exquisitely high signal-to-background ratio with detection efficiency ultimately down to the single-molecule level. (4) Optical sectioning facilitates high-contrast volumetric imaging. (5) Light microscopy allows analysing living systems. These features set optical microscopy apart from other valuable biological imaging approaches, such as electron microscopy (EM), which has exquisite spatial resolution but is incompatible with imaging of living specimens and offers more limited access to molecular information.

[1] johann.danzl@ist.ac.at.

Europe PMC Funders Author Manuscripts

Europe PMC Funders Author Manuscripts

1.1 The diffraction limit

Conventional light microscopes are fundamentally limited in their spatial resolution by diffraction of light waves to about half the wavelength of light or ~200 nm[1–4]. Accordingly, features residing closer to each other than this diffraction resolution limit cannot be discerned, thus preventing the analysis of fine structural details. Many biologically relevant entities, such as cellular organelles or (macro)molecular machineries are assembled on much finer spatial scales. The diffraction limit only applies to “lens-based” microscopy, i.e. methods that operate in the optical “far field”, where the components of the imaging system are positioned at distances from the structure of interest that are large compared to the wavelength of light. In contrast to “near-field” methods[5,6], far-field imaging permits analysing structures inside cells or tissues non-invasively.

1.2 Super-resolution microscopy

Several powerful methods have emerged that break the diffraction resolution limit. Diffraction-unlimited optical “nanoscopy” or “super-resolution” fluorescence microscopy approaches offer spatial resolution that is no longer conceptually limited[7–14]. These methods routinely achieve resolution of tens of nanometers in fixed and living samples and now reach into the single-digit nanometer domain[15,16]. They can be broadly categorized into “coordinate-targeted” methods, such as STimulated Emission Depletion (STED) microscopy, which is the focus of this review, and single-molecule based “coordinate-stochastic” methods. Both rely on preparing fluorophores within a diffraction-limited zone in distinguishable molecular states and reading them out sequentially[7,17]. Any appropriately controllable state transition that turns fluorophores “on” and “off” or, more generally speaking, that renders them distinguishable is suited.

In the single-molecule based methods[8], a sparse subset of fluorophores is activated in each imaging frame and the location of these spatially well separated single molecule emission events is pinpointed with high precision. Thus, a super-resolved image builds up cumulatively from many consecutive imaging frames. These methods include STochastic Optical Reconstruction Microscopy (STORM)[18], (Fluoroescence) PhotoActivation Localization Microscopy (PALM,[19]; fPALM,[20]), and a series of other variants which differ in the precise mechanism of fluorophore activation, e. g. Direct-(d)STORM and Ground State Depletion microscopy followed by Individual Molecule return (GSIDM)[21,22]. Also distinguishing between transiently bound and diffusing molecules in (u)PAINT ((universal) Point Accumulation for Imaging in Nanoscale Topography[23–25]) and DNA-PAINT[26] generates the required sparse highlighting of target molecules.

In coordinate-targeted nanoscopy, a pattern of light determines the regions where fluorescence is allowed to originate from, i.e. where fluorophores reside in a signal-emitting “on”-state, on spatial scales finer than the diffraction limit (Fig. 1). The prototypical example is STED microscopy[27–29]. Here, a light pattern transiently silences fluorophores by stimulated emission except for those residing in the immediate (sub-diffraction vicinity of an intensity minimum, ideally an intensity “zero”. The STED light pattern is spatially overlapped with the excitation light.

In addition, several techniques have pushed the limit of resolution while still remaining conceptually limited by diffraction These do not require on/off switching of fluorophores and hence often offer fast and gentle imaging conditions where only moderate resolution increase over conventional microscopy is required. For example, 4Pi-[30] and I5M-[31] microscopy increase the resolution along the optical (*z*-)axis by exploiting interferometric effects. Structured illumination microscopy in its linear variant yields a resolution enhancement by a factor of two over conventional widefield imaging[32,33]. However, in its nonlinear variant, conceptually unlimited resolution increase is achieved via saturation of fluorophores[34,35].

An interesting alternative super-resolution approach has recently emerged. “Expansion microscopy” increases effective spatial resolution by embedding in and linking the sample to a swellable hydrogel that is then isotropically expanded[36]. Here, rather than increasing optical instrument resolution, the physical separation between fluorophores in the sample is increased. Effective resolution is thus increased, presently down to ~25 nm on conventional light microscopes[37–39]. By design, this method is limited to fixed samples.

In this review, we focus on strategies to improve STED microscopy. We will first briefly recall some of the basic features of the interaction of light with biological matter in fluorescence light microscopy. These considerations apply to diffraction-limited as well as super-resolution microscopy but merit special attention in nanoscale optical imaging because they are more likely to become limiting factors here.

1.3 Interaction of light with biological samples and fluorophores

In fluorescence microscopy, absorption of an excitation light photon by a fluorophore followed by emission of a fluorescence photon is the desired mode of interaction between light and fluorophores (Fig. 1b)[40]. Here, fluorophores are excited from the ground state (typically a singlet state S_0) to the first excited state S_1. The excited state lifetime of fluorescent labels is typically a few nanoseconds (~1-4 ns). The emitted fluorescence light is of longer wavelength because some energy is dissipated via vibrational transitions, leading to a “Stokes shift” between the maxima of excitation and emission spectra.

Direct absorption of light by biological specimens—Many cellular constituents absorb light, which is usually undesired in fluorescence microscopy. Often, absorption cross sections rise for shorter wavelengths. For example, absorption by proteins drastically increases in the blue and UV range due to the presence of aromatic amino acid side chains. Similarly, nucleic acids absorb in the UV. Many further cell and tissue resident chromophores, such as e. g. hemoglobin or cytochrome c, display distinct absorption spectra. All of these lump together to a wavelength-dependent tissue absorption coefficient[41,42] that decreases from the UV/blue to the red/near infrared range, such that long wavelengths prove advantageous for imaging.

Autofluorescence—Along the same lines, some of the cellular constituents not only absorb light but also act as endogenous fluorophores. Although they typically exhibit low quantum yield (i.e. low probability of emitting a fluorescence photon upon excitation) they may collectively contribute a significant undesired background signal, reducing signal-to-

background ratio in fluorescence imaging. Such autofluorescence is often excited more efficiently with blue than with red light, thus again rendering the red to near infrared spectral region an attractive choice for imaging[40]. Endogenous fluorophores typically exhibit short fluorescence lifetime, such that time-resolved fluorescence detection can be useful for suppressing this unwanted background.

Scattering and aberrations—Under ideal conditions, imaging light would traverse the biological specimen in an unperturbed manner as in a perfectly transparent and homogeneous sample of the appropriate refractive index, thus producing an ideal focus in the sample or on the detector. However, scattering of light at refractive index inhomogeneities in biological samples can be a major factor limiting imaging performance in diffraction-limited microscopy but even more so in super-resolution microscopy, especially when aspiring to image deep in tissue samples. While the precise dependence on wavelength varies with the size of the scatterers, there is overall a steep decline of scattering cross section with increasing wavelength[42–44].

Similarly, a mismatch between sample refractive index and the optical design of the objective lens including immersion, as well as spatial variation of the sample's refractive index may induce optical errors (aberrations), deteriorating imaging performance.

Spectral window for imaging—Absorption by most cellular constituents decreases with wavelength, just as scattering does. The absorption cross section of water rises in the near infrared region, thus defining in between a spectral "window" in the red to near infrared region that is often considered desirable for optical imaging[45].

Mechanisms of sample damage—Absorption of light by molecular constituents of cells and tissues or fluorescent labels may lead to physiological or structural alterations of the sample which are particularly of concern when imaging living specimens. The precise mechanisms of sample damage depend on the characteristics of the light exposure. They include direct absorption with covalent bond breakage and radical formation, especially for short wavelength light and deposition of excessive energy leading to thermal damage.

Photobleaching—Fluorophores mediate an important and often dominant part of photodamage. Mechanisms of photobleaching include excitation of fluorophores to higher lying molecular states S_n. From there, they are likely to transition to triplet states T_m ("inter-system crossing") or even dissociate in case they are excited to a non-binding state[46] (Fig. 3a). As fluorophores bleach, radicals are generated that may lead to a reaction cascade involving reactive oxygen species, such as singlet oxygen. These compounds constitute a redox burden and may react with cellular constituents in the vicinity, damaging molecules important to the cell's function. Ultimately this may overwhelm cellular redox buffering and repair mechanisms and lead to irreversible damage and cell death.

Compared to diffraction-limited microscopy, super-resolution imaging with its on/off switching cycles and increased light doses and intensities puts an additional burden on the sample and a higher demand on fluorophores. Clearly, if perturbation of the sample is overwhelming, no informative imaging data can be collected. But also in less severe

situations, bleaching reduces the number of fluorophores available for the measurement and thus decreases signal-to-noise ratio (SNR) and hence the meaningful resolution that can be dialled into a STED measurement[47,48]. Moreover, in order to decode the spatial distribution of target molecules, they must be decorated with fluorescent labels reporting on their positions. The fraction of target molecules associated with a functional fluorophore determines whether they are adequately sampled. Taking into account the sampling theorem, this labelling density is thus a direct determinant for the achievable biologically meaningful resolution, which is again jeopardized by photobleaching.

While there is general consensus that reduction of light exposure and photobleaching is highly desirable[49], systematic studies on the effects of light exposure on (living) biological specimens in super-resolution imaging are relatively sparse. For example, the Sauer group has analysed light exposure effects in single-molecule based super-resolution imaging[50]. For STED microscopy, the Bewersdorf group has recently obtained encouraging results, indicating that a parameter regime can be found where high resolution data can be obtained from living cells such that a substantial fraction of cells remain viable for prolonged periods of time after imaging[51]. These authors also give valuable advice for reducing phototoxicity in live-cell STED nanoscopy. Promising developments are under way that reduce light exposure and/or photobleaching in STED microscopy. For example, a combination of reduced photobleaching and increased on/off state contrast in an approach called “protected STED”[52] enabled decoding the structure of a neuron in a tissue volume of a living brain slice with 3D diffraction-unlimited resolution (Fig. 2). Excitingly, in single-molecule based nanoscopy, efficiency of photon usage previously deemed impossible has been achieved with the MINFLUX concept[15,53].

1.4 Scope of this review: maximizing performance in STED nanoscopy

Super-resolution imaging requires special attention to several factors in order to generate a faithful representation of the specimen. These include sample preparation and labelling approaches, instrument performance, and the specifics of the measurement process itself. There are a range of excellent reviews on STED microscopy that cover various important aspects, e.g. references:[7,11,54–59].

In this review, we first give some basic considerations for optimizing STED measurements. We then put an emphasis on strategies to reduce light exposure as well as photobleaching. Whether perturbation of the sample can be kept at acceptably low levels decisively influences to what extent meaningful information can be obtained from a measurement and the resolution that can be dialled into a STED experiment, especially for obtaining volumetric datasets of biological specimens with super-resolution in all three spatial dimensions. We further discuss correction of optical errors and parallelized, non-point scanning implementations. The latter promise increased acquisition speed of large sample areas and volumes.

2 Principle of STED nanoscopy

In STED nanoscopy, the excitation light distribution is spatially overlapped with an additional STED light pattern that drives fluorophores from the excited state S_1 to the

ground state S_0 via stimulated emission, such that spontaneous emission of a fluorescence photon cannot take place[27,28] (Fig. 1). The STED light thus drives fluorophores to a non-signalling off-state (Fig. 1a)[7]. The photon generated by stimulated emission is of the same wavelength as the STED laser and blocked from detection by optical filters. This additional $S_1 \rightarrow S_0$ pathway effectively outcompetes the spontaneous transition to the ground state[60] if the STED light intensity is sufficiently high. The intensity where a certain fraction of fluorophores (typically defined as 50 %) are turned off is called saturation intensity I_S. It is specific for each combination of fluorophore and STED light characteristics, including STED wavelength.

The STED light distribution features maxima and, crucially, minima that ideally have zero intensity. The shape of the STED light pattern is itself limited by diffraction. However, by increasing the overall power in the STED beam, the saturation intensity is reached near the intensity zero and the STED light pattern is thus able to define on-state and off-state regions on a spatial scale that is finer than the diffraction limit. It sets the coordinates where fluorescence is allowed to originate from directly in the sample.

In most practical realizations, the excitation light takes on the shape of a diffraction-limited laser focus and the STED light distribution features a single intensity minimum with a "doughnut"-shaped light distribution in the focal region (Fig. 1c), resulting in a single-point scanning implementation. Such a doughnut-shaped focus can be created by a 2π-helical phase modulation of the incoming wave front in the back focal plane of the objective lens[61]. Whereas the doughnut beam only increases resolution in the focal plane (*xy*-direction), an additional *z*-STED light pattern ("*z*-doughnut" or "bottle beam", created by a π-phase retardation of the central portion of the beam)[29] may be employed to also increase resolution along the optical axis (*z*-direction). Most practical implementations of single-point scanning STED microscopes are based on a confocal design for facile optical sectioning, but other configurations, such as two-photon (2P) excitation combined with STED, have also been implemented[62–66]. However, a particular geometry is not part of the STED concept. Resolution increase in the *z*-direction can e. g. also be reached with a more elaborate, interferometric 4pi-STED approach[67], which has yielded isotropic 3D STED resolution[68]. The STED light pattern may also be implemented with other light distributions, as long as they feature appropriate intensity zeros, including e. g. highly parallelized or light-sheet based approaches, as discussed in sections 9 and 10.

Resolution in STED nanoscopy

The smallest distance d_0 that can be resolved in a conventional light microscope is approximately $d_0 \approx \frac{\lambda}{2NA}$, where NA is the numerical aperture of the objective lens and λ the wavelength of light. In STED mode, one may approximate the STED light intensity profile around the minimum as a parabola and assume exponential decay of fluorescence ability as a function of STED light intensity. This directly yields a smallest resolvable distance $d \approx d_0 \frac{1}{\sqrt{1 + I_{max}/I_S}}$ with I_{max} being the applied peak intensity[47,61,69,70]. Note that this expression for resolution is no longer fundamentally limited but approaches zero for large values of I_{max} with the lower bound effectively being set by the size of individual

fluorophores (~ 1 nm). Resolution only scales with the square root of I_{max}, such that increasing resolution by applying more STED power becomes progressively harder. This sets practical limits to the achievable resolution in view of photobleaching and finite quality of the STED intensity zero. In fact, the highest resolution STED measurements have been achieved with extremely photostable nitrogen vacancy centers[71].

Beyond this simple consideration, the spatially varying on/off state contrast generated by the STED light pattern directly translates to the effective point spread function (PSF) of the STED microscope (taking also the excitation and detection point spread functions into account)[47,48,52]. The effective PSF corresponds to the instrument response to a point-like emitter in the sample. For example, a diffraction-limited pedestal is created in the effective PSF if fluorophores in designated off-regions have a finite probability for residing in the on-state, e. g. due to spontaneous emission before full action of the STED light or erroneous excitation by STED light from S_0 to S_1 in a process called “Anti-Stokes” excitation. Convolution of such an imperfect effective PSF with the sample structure during image formation may lead to severe degradation of (super-resolution) signal-to-noise ratio and complete loss of super-resolution information in densely packed areas[52]. Therefore, the achieved on/off state contrast is a crucial determinant for performance of STED and other coordinate-targeted super-resolution modalities and is distinct from the common notion of “image contrast” in microscopy.

Timing considerations

The spatially varying on/off state contrast is “written” into the molecular states of the fluorescent labels within a time period shorter than the excited state lifetime of the fluorphores (Fig. 1d). This (sub-) nanosecond timescale is fast compared to the processes we commonly address in biological measurements. STED can hence be used to read out extremely fast biological processes and imaging rates of 125 frames per second have been achieved, limited only by the rate of photon emission from the sample[72]. Even diffusion of a small molecule in solution through a volume corresponding to the diffraction-limited focus generated by a high-*NA* objective takes place on the scale of (tens of) microseconds. Therefore, movement of freely diffusing fluorophores does not lead to appreciable blurring of the locally and “instantaneously” created on/off state contrast. Accordingly, STED is suited to assess the distribution of diffusing dye molecules, both intracellularly[73] and extracellularly[74]. Similarly, in STED-Fluorescence Correlation Spectroscopy (STED-FCS), the STED process is used to confine the observation volume for diffusion measurements to sub-diffraction spatial scales[75]. Signal integration time at each scan position (pixel dwell time) is typically in the (tens of) μs range.

Most STED implementations rely on pulsed lasers for excitation and STED. Excitation pulses are chosen considerably shorter than the excited state lifetime and typically have durations of up to ~100 ps. For 2P-excitation STED microscopy, typically femtosecond excitation pulses are employed, just as in conventional 2P-microscopy[76]. Optimization over the years have shown that STED pulses with a duration of hundreds of ps to ~1 ns are advantageous[77], especially if combined with “time gating” of fluorescence detection to maintain high state contrast, as discussed in the next section. This regime mitigates high

peak photon fluxes that may lead to unwanted photophysical effects and excessive photobleaching. In fact, STED pulses were originally obtained from mode-locked femtosecond lasers and performance increased substantially when pulse stretching via high refractive index glass rods and long optical fibers (~100 m) was introduced. Nowadays, pulsed fiber lasers with the appropriate pulse length are a popular choice.

The excitation pulse sets the time when fluorophores are transferred to S_1. The STED pulse must arrive at the same time as the excitation pulse at the sample in order to drive the transition $S_1 \rightarrow S_0$. Therefore, excitation and STED pulses must be carefully synchronized.

In continuous wave (CW) STED microscopy, STED is implemented with a CW-laser but the excitation laser typically operates as a pulsed laser[78,79]. The CW STED laser obviates the need for pulse synchronization. However, it also entails that in the gaps between excitation pulses the sample is exposed to STED light that does not contribute to image formation. The pulsed excitation again serves to set the time when fluorophores are transferred to the excited state, as required for time gating of fluorescence detection.

Time gating of fluorescence detection

With a precisely defined time point for transfer to S_1, the opportunity arises to synchronize fluorescence detection with excitation, detecting only photons emitted in a selected time window of several nanoseconds duration (Fig. 1d)[80–82]. This is attractive because with long (~1 ns) STED pulses or CW STED, in the initial phase of the action of the STED light, there is a finite probability for spontaneous emission also in designated off-regions. This decreases on/off state contrast and hence signal-to-background ratio and resolution. With time-gated detection, fluorescence photons are collected starting only after full action of the STED light, e. g. ~1 ns after each excitation pulse. Accordingly, photons that were spontaneously emitted in designated off regions before full action of the STED light are preferentially rejected, thus increasing on/off state contrast. The detection window is closed after most of the fluorescence emission has taken place (e. g. after ~10 ns, corresponding to a few fluorescence lifetimes). Time gating can also be helpful for rejecting autofluorescence and, especially in low repetition rate implementations, noise from technical sources or stray light.

Multi-colour and co-localization measurements

Super-resolution optical imaging is uniquely positioned to investigate spatial relationships between different molecules. In STED microscopy, combinations of two[77,83], three[84,85], or four[86] fluorophores are available that can be addressed with the same STED beam but distinguished in their emission and/or excitation properties. In this configuration, one and the same STED light intensity minimum sets the fluorescence emission coordinates for all fluorophores simultaneously, thereby abrogating all alignment and magnification errors between colour channels. This facilitates high-confidence co-localization studies with minimized systematic errors.

Generalization of the concept

The STED approach has been generalized to any appropriately light-addressable molecular transition making fluorophores distinguishable in the framework of the “REversible

Saturable Optical Fluorescence Transitions" (RESOLFT) concept[69,87–89]. Specifically, switching between the metastable on- and off-states of dedicated reversibly photoswitchable fluorophores has made coordinate-targeted nanoscopy at low light intensities with long observation times possible[90]. Compared to STED, the long timescales associated with photoswitching (commonly hundreds of microseconds photoswitching time at each scan position) bear the advantage that low light intensities are sufficient to drive the off-transition but come with the drawback of reduced imaging speed. The ~100 μs- to ms-timescale for generating state contrast means that this approach at present is not suitable for imaging with rapidly diffusing molecules as labels. Reversibly photoswitchable fluorescent proteins (RSFPs)[91–93] and fluorescent dyes[94–97] are undergoing intense development with intriguing prospects for the future.

3 Basic considerations for optimizing performance in STED nanoscopy

STED nanoscopy is straightforward in terms of data acquisition and analysis as it directly generates super-resolved images without the need for sophisticated data processing. However, for satisfactory performance it needs care in instrument and experiment design. While imaging of a single or a few planes with resolution increase only laterally is typically easy to accomplish, requirements in terms of repeated imaging capability and reduction of sample light exposure are much more stringent if one aspires to reconstruct an entire volume of a cell or tissue with resolution enhancement in all three spatial directions.

In particular, the following basic considerations help avoid loss of signal and excessive fluorophore bleaching.

(1) The major factor determining whether fluorophores residing in a designated on-region generate signal is the quality of the intensity zero. Any non-zero STED light intensity I_{min} at the minimum effectively turns off fluorophores. For example, if $I_{max}/I_S \approx 100$ for ~10-fold resolution increase, already 1% of peak intensity leaking into the intensity minimum would mean $I_{min} = I_S$, reducing fluorescence signal by half. Any loss of signal requires additional excitation intensity or integration time to recover the signal-to-noise ratio, increasing light burden on the sample potentially up to a parameter regime where excessive photobleaching effectively precludes recording of high resolution data. The quality of the intensity minimum of an *xy*-STED doughnut is critically influenced by (i) the polarization of the STED light, which must be perfectly circular and match the helicity of the phase ramp used to generate the doughnut-shaped light distribution; (ii) sample-induced scattering of STED light into the intensity minimum, limiting tissue penetration; (iii) optical aberrations of the STED beam induced by the optical system or the sample; (iv) and a spectral width of the STED laser beyond ~10 nm may become problematic as different wavelengths may form their intensity minima at slightly offset spatial positions, eliminating an overall intensity zero. For other STED light distributions, different considerations apply. The quality of the intensity zero of a *z*-STED pattern ("*z*-doughnut") is exquisitely sensitive to spherical aberration, an optical

error that frequently arises due to refractive index mismatch between the sample and the immersion medium/objective lens design.

(2) State cycling takes place in regions where both excitation light and STED light are present. In a perfectly aligned STED microscope, the intensity minimum of the STED light pattern and the intensity maximum of the excitation focus coincide. Any slight misalignment causes the excitation maximum to coincide with regions of higher STED intensity, leading to loss of signal, excessive state cycling, and photobleaching.

(3) The STED process is exquisitely sensitive to timing of excitation and STED pulses on the sub-ns timescale. Incorrect timing or timing jitter leads to reduced action of the STED light, thus sacrificing state contrast and resolution for a given STED light exposure. Equally, correct setting of detection time gating maximizes state contrast and hence information for a given light dose.

(4) The STED wavelength is typically chosen in the long wavelength tail of the emission spectrum of the fluorophore. The choice of STED wavelength is governed by two opposing factors: wavelengths close to the emission maximum increase the cross section for stimulated emission[98] and reduce the intensity required to achieve a given resolution. However, with decreasing STED wavelength, the probability for directly exciting fluorophores ($S_0 \rightarrow S_1$) via Anti-Stokes excitation increases, thus deteriorating on/off-state contrast.

(5) STED light may drive additional photophysical processes depending sensitively on the fluorophore's energy structure, which is, however, typically not well characterized spectroscopically[99]. STED light may excite a fluorophore from the ground state in a single- or two-photon process or drive excited state absorption from S_1 to higher lying molecular states S_n. Fluorophores may transition to triplet states via inter-system crossing where they may also absorb STED light (triplet state absorption) and may populate higher lying triplet states T_m. Therefore, resistance to photobleaching and overall imaging performance may differ considerably between STED vs. diffraction-limited mode and among fluorophores. The choice of fluorophore requires testing under STED conditions, for which further systematic studies would be desirable. Long STED pulses (~1 ns) lead to lower peak pulse intensities, mitigating unwanted processes that depend non-linearly on intensity, such as two-photon transitions driven by the STED laser.

(6) Last but not least, sample light exposure, photobleaching and thus overall imaging performance can be optimized most easily by a prudent choice of imaging parameters. In STED microscopy, resolution scales with the square root of the applied intensity. Hence, it gets quadratically harder to "squeeze out" additional resolution and marginal benefit of higher STED power decreases. Following the sampling theorem, increased resolution also requires smaller step size for scanning (smaller pixel size). Light exposure scales quadratically with the inverse pixel size for acquiring a single plane. Similarly, excessive oversampling with smaller than necessary pixel size should be avoided.

4 Labeling is a decisive factor for STED microscopy performance

4.1 Sample preparation and choice of fluorophores

The quality of sample preparation profoundly influences the imaging outcome. Evidently, any shortcomings of fixation or labeling procedures, such as nanoscale distortions of the sample structure from chemical fixation, are much more evident and more limiting in super-resolution imaging than in diffraction-limited microscopy and often warrant optimization and specialized protocols. Sufficiently high labelling density is central to resolving a structure of interest. In addition, the labelling strategy may entail a "linkage error", i.e. a spatial displacement between target molecules and fluorophores. Specifically, the size of primary and secondary antibodies (each ~ 10 nm) in immuno-stainings leads to errors that are substantial on the scale of the resolution currently achieved in super-resolution imaging. Smaller probes, like e. g. nanobodies, promise more accurate reporting on target molecule positions[100]. Specificity of labeling has a major influence on signal-to-background ratio, which is a key determinant of STED performance.

Fluorescent proteins, like green fluorescent protein (GFP) have been employed in STED[101]. However, broadly speaking, high performance synthetic fluorescent dyes offer higher photostability and photon budgets, i.e. number of emitted photons before photobleaching, than fluorescent proteins. Therefore, it is advisable to use fluorescent dyes as labels for STED if possible. Also for live imaging, an increasing palette of synthetic dyes is becoming available[102–106]. These can be targeted to specific molecules of interest via a range of methods, such as SNAP tag[107], Halo tag[108], click chemistry[109], or small peptide tags[110]. Fluorescent proteins can also be highlighted with dye-coupled specific antibodies or nanobodies[111].

Imaging buffers that scavenge reactive oxygen species may further improve performance in STED microscopy[51,112]. An intriguing development are "self-healing" dyes with protective groups[113–118].

4.2 Replenishment of fluorophores facilitates repeated imaging

A simple strategy for mitigating the effect of photobleaching on the imaging outcome is to replenish bleached fluorophores during the imaging process. Dissociation of affinity binders with moderate affinity frees the binding site after photobleaching for another binder carrying a new label, thus constantly turning over flurophores. A good example is the actin binding peptide Lifeact[119], which has been used to reconcile molecular specificity with replenishment of fluorophores in STED imaging of neuronal structures[120]. Similarly, replenishing membrane stains profit from fluorophore turnover[121]. Fluorophore-conjugated DNA-oligonucleotides that bind to complementary barcoding sequences introduced into the sample during labelling can also be used for exchanging fluorophores[122–125].

Fluorophore replenishment is particularly easy to implement if fine morphological features, rather than molecular arrangements, are of interest. A prototypical example is STED-based analysis of the elaborate shapes of dendritic spines, the postsynaptic specializations of many excitatory synapses in the central nervous system, in living neurons expressing a fluorescent

protein in the cytosol[73]. Similarly, single neurons or other cells can be accessed in whole cell mode with a patch clamp pipette filled with a dye containing solution.

A similar approach can also be applied for staining the extracellular rather than intracellular spaces. Here, cellular structures are demarcated as "shadows" in the bath of extracellularly applied dye, hence the term "SUper-resolution SHadow Imaging" (SUSHI)[74]. This has yielded fascinating images of the architecture of neuronal tissue. Also here, bleached dye molecules are simply substituted with fresh ones by diffusion.

It should be noted that replenishment of fluorophores does not reduce photobleaching, but rather the effect of photobleaching on image quality. If fluorophores bleach, they create the same radicals, metabolic burden and photochemical damage as with other labelling strategies, albeit with different implications for intra- and extracellularly generated toxic products.

In these approaches, sample light exposure remains unaltered in first approximation. Therefore, direct absorption of the imaging light by the tissue is still equally of concern. However, in some cases, such as bath application of fluorophores, the local concentration of fluorophores can be set very high, such that low excitation power and/or short pixel dwell times are sufficient to collect enough signal.

5 Dark/triplet state relaxation increases the photon budget

During repeated excitation and (stimulated) emission cycles, fluorophores may transition to the triplet manifold by inter-system crossing (Fig. 3a). Fluorophores residing in triplet states are "dark" and do not contribute to signal generation. However, they are typically not inert. They may still absorb excitation or STED light, causing excitation to higher lying triplet states, and undergo chemical reactions[46]. A typical outcome is the formation of radicals that react with cellular targets and damage them permanently.

Evidently, it is desirable to keep fluorophore population in triplet/dark states low. Triplet states are typically long-lived and the fraction of fluorophores residing in dark states depends on the rates at which they are pumped there and at which they relax back to the singlet manifold, which differ between fluorophores for given light exposure.

There is a simple and general strategy to minimize dark/triplet state population: Allowing time in the imaging procedure for fluorophores to relax back to the singlet manifold, with relaxation timescales on the order of ~1 μs. This is applicable both to diffraction-limited[126] and super-resolution STED imaging[127] and leads to substantial signal increase and reduced bleaching.

Strategies to increase dark state relaxation include (i) low repetition rate excitation, (ii) fast scanning with accumulation of the signal over individual image lines or frames that are repeatedly queried, and (iii) dedicated short breaks during image acquisition without light exposure.

Low repetition rate gives fluorophores time to relax between individual excitation events. The original implementation demonstrated a significant improvement at 250 kHz over 80 MHz pulse repetition rate[127], albeit at correspondingly increased acquisition times. However, also higher, more user-friendly pulse repetition rates in the low to ~20 MHz range seem to offer an improvement over e. g. the 80 MHz typically dictated by mode-locked titanium:sapphire lasers.

Fast scanning has been implemented with a range of technologies: In STED, resonant mechanical scanners have been employed early on[79,128], achieving video-rate nanoscopy. Here, lines are queried repeatedly and signal is accumulated. Scanning without mechanically moving parts further increases scan speed. Acousto-optical scanning[129], where scan speed is limited by travelling times of acoustic waves, enabled triplet state relaxation in conventional 2P-microscopy. Even faster scanning is possible via electro-optical scanners, such that signal can be accumulated frame-wise with maximized triplet state relaxation until the desired signal-to-noise ratio is reached[72].

Even with a conventional scanner based on galvanometric mirrors, dividing up the total acquisition time for each scan position by accumulating several line scans of shorter duration or brief laser blanking at each scan position may yield an improvement of the imaging outcome.

6 Adaptive illumination strategies reduce overall light exposure

Light exposure can be significantly reduced if excitation and STED illumination are only applied as necessary to obtain the desired information or resolution. This simple thought forms the basis for several related techniques.

In RESCue (REduction of State transition Cycles) STED, the fluorescence photon counts are compared to user-set thresholds during acquisition[130] (Fig. 3b). If the photon count at a scan position does not exceed a lower threshold after a predefined fraction of the acquisition time, it is set to zero assuming that no emitter is present. For bright signals surpassing an upper threshold at any time during acquisition, the photon count can be extrapolated to the remaining dwell time while maintaining sufficient SNR. In both cases, all lasers are turned off for the remaining dwell time to spare the sample from unnecessary light exposure; only if neither case applies, acquisition continues for the full dwell time. Reliably deciding between the three scenarios requires a certain number of photons. Still, depending on sample structure, sizeable reductions in light dose and photobleaching may be achieved, with largest benefits for bright and sparse samples (Fig. 4). The RESCue approach is adapted from previous developments in confocal microscopy[131] and has also been applied to RSFP-based RESOLFT[132].

In DyMIN (DYnamic intensity MINimum) STED[133], full STED power is only applied where high resolution is required. Only if fluorescence is detected in the diffraction-limited probe step, the STED laser is turned on to silence fluorophores at the periphery of the excitation volume. If signal is still emitted from the smaller volume, STED power (P_{STED}) is consecutively stepped up to narrow the effective PSF until the desired resolution is reached.

If, on the other hand, no signal is collected, a further power increase would not yield additional information. Probe steps could e. g. be $P_{STED} = 0$ for diffraction-limited resolution, $P_{STED} = P_{max}/4$ for ~ half the final resolution, and the highest STED power P_{max} for maximum resolution. Significant reductions in STED light exposure can be achieved, potentially sparing sample regions that do not contain structures of interest from intense STED exposure.

In “multilevel STED”, the STED illumination intensity for multicolour imaging is adjusted according to the requirements for each (spectrally distinct) fluorophore to achieve the same resolution, given differing cross sections for stimulated emission at a fixed STED wavelength[85].

For sub-micrometer-sized regions of interest, the scan range can be narrowed down such that the high-intensity crest of the STED doughnut remains outside and never scans across the nanoscale structures of interest (MINFIELD STED, Fig. 3d, Göttfert et al. [134]). Increasing the total power of the STED beam steepens the gradient around the intensity minimum and improves resolution.

7 Multiple off-state transitions for protecting fluorophores

The realization that fluorophores and other labels are not just passive “colouring agents” but offer a molecular state structure that can be manipulated and therefore harnessed to improve imaging was the key to breaking the diffraction limit[12]. STED is the paradigmatic example for fluorophores being deterministically transferred between a signalling on-state and a non-signalling off-state. Similarly, switching between an off- and an on-state lies at the heart of the single-molecule based super-resolution techniques.

While controlling a single off-transition is sufficient for nanoscopy, controlling multiple state transitions opens up refined manipulation of molecular states and synergistic action for diffraction-unlimited image generation. In multiple off-state transitions (MOST) nanoscopy, two (or more) off-state transitions are exploited to generate the on/off state contrast required for coordinate-targeted nanoscopy[52]. In its prototypical implementation as “protected STED” (Fig. 5), the two off-state transitions were realized by stimulated emission, as in conventional STED microscopy, and reversible photoswitching in RSFPs. This scheme has two important implications:

1. It introduces a second off-state OFF_2. If appropriately chosen, transfer to this state protects fluorophores from photobleaching associated with high STED light intensities, thus increasing repeated imaging capability.
2. When two independent off-transitions act to define on- and off-regions, the achievable on/off state contrast is higher due to synergistic action of the two off-transitions.

In protected STED, fluorophores are pre-emptively transferred to OFF_2 in regions of high STED light intensity before applying the combined excitation and STED pulses. Fluorophores in these regions are still exposed to the high STED light intensities but as they reside in OFF_2 they essentially do not interact with the STED (and excitation) light (Fig. 5c).

They are hence spared from repeated excitation/stimulated emission cycles and unwanted photophysical processes. This translates into reduced photobleaching and increased repeated imaging capability (Fig. 5e). A further effect contributes to reduced photobleaching: In first approximation, both off-transitions take equivalent roles for increasing resolution and their relative contribution can be tuned at will. Therefore, STED power can be reduced while still taking advantage of the improved state contrast over nanoscopy using reversible photoswitching as a single off-transition.

Improved state contrast is easily rationalized when modelling the effective PSF[52]. It is instructive to first briefly recall the situation with a single off-transition. Any off-transition is expected to suffer from some imperfection in creating on/off state contrast, corresponding to a finite population of fluorophores in the signalling state also in designated off-regions. In STED nanoscopy, this might arise from spontaneous emission before the STED light can take full action or from Anti-Stokes excitation, wheras in RESOLFT nanoscopy with photoswitchable fluorophores, “photoswitching background” arises from incomplete transfer to or spontaneous return from the deactivated configuration. Imperfect state contrast directly leads to a diffraction-limited pedestal in the effective PSF in addition to the desired sharp peak. During image generation in the microscope, the sample structure is convolved with the effective PSF, where, especially in dense regions of the sample, summation over these diffraction-limited components severely reduces (super-resolved) signal to (diffraction-limited) background ratio and hence the achievable resolution. In contrast, if also a second off-transition is operative, the situation changes. The effective PSF is just the product of the individual spatially varying probability distributions for assuming the on-state associated with each of the individual on- and off-state transitions and also the detection PSF. This product implies that a diffraction-limited pedestal left from one off-state transition is counteracted by multiplication with the probability distribution of sub-diffraction width stemming from the other off-transition. The combination of repeated imaging capability and enhanced state contrast enabled 3D super-resolved imaging of volumes of living brain tissue where individual neurons were highlighted and reconstructed in 3D (Figure 2).

Several prerequisites have to be fulfilled for protected STED. Trivially, the fluorophore must be a sufficiently good STED label to begin with. Similarly, it must sustain a large number of on/off photoswitching cycles, i.e. low “switching fatigue” for the second off-transition to be protective against photobleaching. STED light should not be absorbed by the putatively protective off-state OFF_2. In addition, the state transitions must be sufficiently decoupled from each other. For example, the intense STED laser could in principle drive a two-photon transition from the deactivated to the activated configuration, jeopardizing the protective effect. However, the ns-laser pulses of a STED laser are expected to drive two-photon transitions much less efficiently than the femtosecond pulses typically used for 2P-excitation or 2P-uncaging. For the reversibly photoswitchable GFP (rsEGFP) variants[90,91,135], 2P-activation by STED light was negligible in typical imaging parameter regimes. In the initial proof-of concept, protected STED has only been realized with rsEGFPs. However, the protective effect per se is also present in other reversibly photoswitchable fluorophores[52]. An intriguing prospect for the future are improved reversibly photoswitchable synthetic fluorophores[94–97], which promise increased photostability and photon budgets over fluorescent proteins also for protected STED.

One drawback of protected STED over conventional STED is the requirement for additional light pulses for fluorophore activation and deactivation. While the deactivation step can be chosen shorter than in RSFP-based RESOLFT nanoscopy, it still introduces a prolonged pixel dwell time as compared to conventional STED. An obvious route to increase imaging speed is through parallelization (see section 9).

8 Adaptive optics for correcting optical errors

Aberrations (optical errors) degrade image quality and can be introduced both by imperfections in the microscope's optics ("system aberrations") or by refractive index mismatch and inhomogeneity in the sample. In diffraction-limited microscopy, aberrations prevent the formation of a tight focus, spreading the signal across a larger volume and ultimately degrading signal-to-noise ratio and image contrast. STED microscopy is considerably more susceptible to aberrations. They deform the shape of the light distributions and both aberrations and scattering divert laser intensity into STED light minima.

Aberrations adversely affect STED microscopy in several unique ways: (1) Achievable state contrast and resolution depend critically on the quality of the intensity minimum. A non-zero intensity minimum will decrease signal, elicit unnecessary state cycling, and increase photobleaching. Increasing laser power or acquisition time to counteract low signal-to-noise ratio will worsen detrimental effects further. (2) Spreading of the excitation and STED light patterns may increase their overlap, resulting in increased state cycling and photobleaching. (3) Deformations of excitation and/or STED light patterns may result in regions of insufficient fluorescence suppression, leading to sidelobes and artefacts in the final image.

The effects of aberrations on both the STED light distribution[136] and the effective PSFs[137] have been studied computationally. Notably, coma aberrations in a 3D STED system lead to a translation of the intensity minima for the *xy*-doughnut and *z*-STED pattern in opposing directions, resulting in non-overlapping minima and signal loss in an otherwise perfectly-aligned system[138].

Spherical aberrations in STED microscopy can often simply be minimized by using an objective lens and immersion medium matched to the sample refractive index, e. g. with glycerol[120,139] or water objectives[140] normally also featuring a correction collar.

Adaptive optics approaches promise to restore image quality in aberrating samples and are an area of active development in various fields of microscopy[141]. Here, an active optical element (e. g. deformable mirror, DM or spatial light modulator, SLM) is used to pre-compensate system- and sample-induced aberrations. The same devices can potentially be used to additionally imprint phase patterns onto the wavefront to emulate discrete optical elements, including the phase masks for forming *xy*- and *z*-STED patterns. At present, many STED implementations use an SLM instead of conventional (polymer) phase masks to shape the STED light patterns, such that the same SLM can be used for correction of system or sample-induced aberrations without any additional optical elements or intensity losses. The STED patterns are the main determinant for image contrast and resolution, such that here

aberrations are more problematic than for the regularly focused excitation foci. Already with a single SLM, both the STED *xy*-doughnut and the *z*-STED light pattern can be generated and corrected for system aberrations[142]. The same hardware can also be used to execute an auto-alignment routine overlaying the excitation and depletion beams[143].

Excitation beams can be corrected either by adding an additional SLM to the excitation path[144], by passing both excitation and STED beams over a common DM[145] or by a double-pass geometry where the same SLM is used to correct both excitation and STED beams[146].

Clearly a major challenge in adaptive optics is to determine the correction pattern to dial in. Two principal approaches exist: (1) measuring the wavefront directly or (2) iteratively optimizing an image quality metric while different corrections are applied. The first requires a high signal-to-noise measurement of sample-induced aberrations from the dim fluorescence signal; the second necessitates multiple measurements on the sample during the optimization process. Therefore, either approach subjects the sample to additional light exposure, potentially prematurely bleaching it.

9 Parallelization of image acquisition

Single-point scanning is the most wide-spread implementation of STED microscopy, usually combined with confocal detection. Here, the necessary STED light intensities are reached with readily available laser sources and optical sectioning is achieved with a comparatively simple optical setup. With its action on the (sub-)ns timescale, the STED process itself is extremely fast. However, point scanning limits high-speed recordings to small fields of view.

Parallelization by reading out from many STED light intensity minima simultaneously is an attractive route towards high-speed super-resolution imaging of large fields of view. In an initial implementation, both the illumination and STED beams, as well as detection, were multiplexed four-fold[147]. Considerably higher degrees of parallelization have been achieved using standing wave patterns. They can be created in the focal plane by interfering a pair of laser beams focused off-axis through the objective. Incoherently superimposing two perpendicular standing waves results in an optical lattice featuring a periodic pattern of thousands of intensity minima and maxima as used for STED[148,149]) or over a hundred-thousand for RSFP-based RESOLFT[135]). Conveniently, the optical lattice setup can be designed such that it is achromatic, facilitating colour multiplexing[150]. For parallelized readout, a high-speed camera is used and the optical lattice is scanned across one unit cell (spanning one period of the lattice) to build a super-resolved image. In highly parallelized STED[148,149], the available laser power is spread across large areas, thus limiting the achievable degree of parallelization for a given target resolution. Reversible photoswitching in RESOLFT[135] offers an advantage because it requires only low light intensities. Similarly, protected STED is expected to facilitate large scale parallelization. Here, improved on/off state contrast and resolution are achieved already at low STED light intensities[52] due to the synergistic contribution of both off-transitions. Accordingly, while the availability of high-power lasers is a limiting factor for parallelization in STED, this requirement would be substantially reduced in parallelized protected STED.

In addition to increased imaging speed, the use of standing waves has two important implications: (1) They provide an up to 15-fold steeper slope around intensity minima and hence require lower peak intensity I_{max} than the prevalent doughnut implementation[149]. (2) Each maximum borders several intensity minima and thus contributes to confining fluorescence in more than a single location.

In parallelized approaches, excess state cycling can be decreased if also the excitation light is patterned[148,150–152], such that the STED light intensity maxima coincide with the minima of the excitation pattern.

Yet, crosstalk between the closely spaced intensity minima makes it necessary to restrict signal collection by the camera to the central pixels corresponding to the intensity minima, resulting in tight “digital” pinholes (e. g. ~ 1/5 of an Airy disk[135]). The pinhole diameter can be increased to transmit more signal if a sparsely spaced (excitation or) photoactivation pattern, matching the diffraction limited resolution, is used, e. g. activating only at every fourth minimum of the off-switching pattern in RSFP-based RESOLFT[153], albeit at the expense of slower acquisition because the patterns have to be scanned across the larger unit cell, now determined by the photoactivation pattern periodicity.

Despite offering massive parallelization in the image plane, existing implementations based on optical lattices achieve only diffraction-limited resolution along the optical axis. Interference with a fifth, on-axis beam has been suggested for resolution enhancement in 3D[154], but experimental demonstration is still lacking.

10 Light-sheet implementations of STED and RESOLFT

In light sheet fluorescence microscopy, a plane of the sample is selectively illuminated with a thin sheet of light, providing optical sectioning and sparing the remainder of the sample from unnecessary light exposure. Light sheet microscopy thus ensures fast, gentle, and high-contrast fluorescence imaging. Light sheets are created either by focusing with a cylindrical lens (“static” light sheet,[155]), by scanning a laser beam rapidly through the sample, resulting in a “virtual” sheet[156], or more elaborate schemes, such as designing the light pattern in the back focal plane of the objective lens to achieve a “lattice” light sheet[157]. Resolution perpendicular to the light sheet, i.e. axially with respect to the detection objective, is governed by the product of the PSF of the detection objective and the light sheet.

To achieve axial super-resolution, light sheet illumination has been combined with STED and RSFP-based RESOLFT: A “hollow” light sheet silences fluorophores above and below the central plane, reducing the effective sheet thickness. A STED implementation demonstrated up to 2.5 fold increased axial resolution[158,159], whereas 5–12 fold improved axial resolution was reported using RSFP-based RESOLFT[160]. Lateral resolution was unaltered and determined by the PSF of the detection objective.

Due to the diffractive nature of Gaussian beams, light sheet thickness and size of the field of view are interlinked. The use of (theoretically) non-diffracting Bessel beams for light sheet generation promises not only larger uniformly-illuminated field of views, but, equally importantly, also less susceptibility to scattering due to the self-reconstructing nature of

Bessel beams[161,162]. Several approaches to suppress the Bessel beam's sidelobes while maintaining its self-reconstructing properties have been demonstrated[163,164]. Simulations have shown that the Bessel beam's sidelobes can also be efficiently suppressed using stimulated emission[165] while retaining the self-reconstructing ability in scattering samples[166]. An initial experimental demonstration has achieved a twofold resolution enhancement[167].

11 Outlook

STED microscopy has come a long way in the last decades: The concept was first proposed 25 years ago and experimentally demonstrated soon thereafter. Since then, STED has undergone a dramatic evolution in terms of performance, ease of use, and accessibility for non-expert labs. It has been serving as a valuable tool for biological research and will do so even more in the future. In this endeavour, each advancement in imaging technology will help to address a new class of biological problems.

Enabling progress is expected in various aspects of STED nanoscopy and other super-resolution techniques. As optical resolution will further increase, ever finer macromolecular arrangements inside cells will become accessible. It will be exciting to visualize these directly in the native spatial context, with cells residing in their complex natural 3D tissue environments. For specific questions, this promises more trustworthy biological data than obtainable from cells artificially grown on a coverslip and incentivizes further super-resolution developments towards 3D-tissue imaging and increased depth penetration. It will be equally exciting to see continued progress in nanoscale imaging of living specimens to follow the dynamic evolution of the biological system. For this, further development of strategies to reduce light exposure, photobleaching, and phototoxicity in live-cell nanoscopy are in high demand. This in turn will boost 3D-diffraction-unlimited analysis of entire tissue volumes. Here, for live measurements, as well as for sufficiently high throughput in fixed tissue analysis, further development of parallelized approaches promises to deliver the required increase in acquisition speed. In parallel to advancing new imaging concepts and developments on the instrumentation side, substantial gain can be expected from new developments in labelling technology. Here, augmented brightness, photostability, and physicochemical properties of the labels will be important catalysts for progress, both for fixed and living specimens. New approaches to multicolour super-resolution imaging will provide high content of molecular information for decoding the three-dimensional nanoarchitecture of cells and tissues. These examples serve to illustrate that a range of exciting developments are on the horizon and we can expect that they will drive fascinating biological discoveries.

Acknowledgements

J.G.D. and P.V. gratefully acknowledge funding by the Austrian Science Fund (FWF; I 3600-B27). W.J. gratefully acknowledges funding by a Human Frontier Science Program long term fellowship (HFSP LT000557/2018).

Europe PMC Funders Author Manuscripts

References

[1]. Abbe E. Beiträge zur Theorie des Mikroskops und der mikroskopischen Wahrnehmung. Archiv für Mikroskopische Anatomie. 1873; 9:413–468. DOI: 10.1007/bf02956173

[2]. Verdet, E. Leçons d'optique physique. Vol. 1. Victor Masson et fils; Paris: 1869.

[3]. Rayleigh JW. On the theory of optical images, with special reference to the microscope. Philosophical Magazine. 1896; 5(42):167–195. DOI: 10.1080/14786449608620902

[4]. von Helmholtz H. Die theoretische Grenze für die Leistungsfähigkeit der Mikroskope. Ann Phys Chem. 1874:557–584.

[5]. Ash EA, Nicholls G. Super-resolution aperture scanning microscope. Nature. 1972; 237:510–512. DOI: 10.1038/237510a0 [PubMed: 12635200]

[6]. Betzig E, Trautman JK, Harris TD, Weiner JS, Kostelak RL. Breaking the diffraction barrier – optical microscopy on a nanometric scale. Science. 1991; 251:1468–1470. DOI: 10.1126/science.251.5000.1468 [PubMed: 17779440]

[7]. Hell SW. Microscopy and its focal switch. Nature Methods. 2009; 6(1):24–32. DOI: 10.1038/nmeth.1291 [PubMed: 19116611]

[8]. Huang B, Babcock H, Zhuang X. Breaking the diffraction barrier: super-resolution imaging of cells. Cell. 2010; 143:1047–1058. DOI: 10.1016/j.cell.2010.12.002 [PubMed: 21168201]

[9]. Toomre, Derek; Bewersdorf, Joerg. A new wave of cellular imaging. Annual Review of Cell and Developmental Biology. 2010; 26(1):285–314. DOI: 10.1146/annurev-cellbio-100109-104048

[10]. Liu, Zhe; Lavis, Luke D; Betzig, Eric. Imaging live-cell dynamics and structure at the single-molecule level. Molecular Cell. 2015; 58(4):644–659. DOI: 10.1016/j.molcel.2015.02.033 [PubMed: 26000849]

[11]. Sahl, Steffen J; Hell, Stefan W; Jakobs, Stefan. Fluorescence nanoscopy in cell biology. Nature Reviews Molecular Cell Biology. 2017; 18(11):685.doi: 10.1038/nrm.2017.71 [PubMed: 28875992]

[12]. Hell SW. Nanoscopy with focused light (Nobel Lecture). Angewandte Chemie International Edition. 2015; 54(28):8054–8066. DOI: 10.1002/anie.201504181 [PubMed: 26088439]

[13]. Betzig, Eric. Single molecules, cells, and super-resolution optics (Nobel Lecture). Angewandte Chemie International Edition. 2015; 54(28):8034–8053. DOI: 10.1002/anie.201501003 [PubMed: 26087684]

[14]. Moerner WE. Single-molecule spectroscopy, imaging, and photocontrol: foundations for super-resolution microscopy (Nobel Lecture). Angewandte Chemie International Edition. 2015; 54(28):8067–8093. DOI: 10.1002/anie.201501949 [PubMed: 26088273]

[15]. Balzarotti, Francisco; Eilers, Yvan; Gwosch, Klaus C; Gynnå, Arvid H; Westphal, Volker; Stefani, Fernando D; Elf, Johan; Hell, Stefan W. Nanometer resolution imaging and tracking of fluorescent molecules with minimal photon fluxes. Science. 2016; 355(6325):606–612. DOI: 10.1126/science.aak9913 [PubMed: 28008086]

[16]. Dai, Mingjie; Jungmann, Ralf; Yin, Peng. Optical imaging of individual biomolecules in densely packed clusters. Nature Nanotechnology. 2016; 11:798–807. DOI: 10.1038/nnano.2016.95

[17]. Hell, Stefan W. Far-field optical nanoscopy. Science. 2007; 316(5828):1153–1158. DOI: 10.1126/science.1137395 [PubMed: 17525330]

[18]. Rust, Michael J; Bates, Mark; Zhuang, Xiaowei. Sub-diffraction-limit imaging by stochastic optical reconstruction microscopy (STORM). Nature Methods. 2006; 3(10):793–796. DOI: 10.1038/nmeth929 [PubMed: 16896339]

[19]. Betzig E, Patterson GH, Sougrat R, Lindwasser OW, Olenych S, Bonifacino JS, Davidson MW, Lippincott-Schwartz J, Hess HF. Imaging intracellular fluorescent proteins at nanometer resolution. Science. 2006; 313(5793):1642–1645. DOI: 10.1126/science.1127344 [PubMed: 16902090]

[20]. Hess, Samuel T; Girirajan, Thanu PK; Mason, Michael D. Ultra-high resolution imaging by fluorescence photoactivation localization microscopy. Biophysical Journal. 2006; 91(11):4258–4272. DOI: 10.1529/biophysj.106.091116 [PubMed: 16980368]

[21]. Heilemann M, van de Linde S, Schüttpelz M, Kasper R, Seefeldt B, Mukherjee A, Tinnefeld P, Sauer M. Subdiffraction-resolution fluorescence imaging with conventional fluorescent probes. Angewandte Chemie International Edition. 2008; 47:6172–6176. DOI: 10.1002/anie.200802376 [PubMed: 18646237]

[22]. Fölling J, Bossi M, Bock H, Medda R, Wurm CA, Hein B, Jakobs S, Eggeling C, Hell SW. Fluorescence nanoscopy by ground-state depletion and single-molecule return. Nature Methods. 2008; 5:943–945. DOI: 10.1038/nmeth.1257 [PubMed: 18794861]

[23]. Sharonov A, Hochstrasser RM. Wide-field subdiffraction imaging by accumulated binding of diffusing probes. Proceedings of the National Academy of Sciences. 2006; 103(50):18911–18916. DOI: 10.1073/pnas.0609643104

[24]. Giannone, Gregory; Hosy, Eric; Levet, Florian; Constals, Audrey; Schulze, Katrin; Sobolevsky, Alexander I; Rosconi, Michael P; Gouaux, Eric; Tampé, Robert; Choquet, Daniel; Cognet, Laurent. Dynamic superresolution imaging of endogenous proteins on living cells at ultra-high density. Biophysical Journal. 2010; 99(4):1303–1310. DOI: 10.1016/j.bpj.2010.06.005 [PubMed: 20713016]

[25]. Lew MD, Lee SF, Ptacin JL, Lee MK, Twieg RJ, Shapiro L, Moerner WE. Three-dimensional superresolution colocalization of intracellular protein superstructures and the cell surface in live *Caulobacter crescentus*. Proceedings of the National Academy of Sciences. 2011; 108(46):E1102–E1110. DOI: 10.1073/pnas.1114444108

[26]. Jungmann, Ralf; Steinhauer, Christian; Scheible, Max; Kuzyk, Anton; Tinnefeld, Philip; Simmel, Friedrich C. Single-molecule kinetics and super-resolution microscopy by fluorescence imaging of transient binding on DNA origami. Nano Letters. 2010; 10(11):4756–4761. DOI: 10.1021/nl103427w [PubMed: 20957983]

[27]. Hell, Stefan W; Wichmann, Jan. Breaking the diffraction resolution limit by stimulated emission: stimulated-emission-depletion fluorescence microscopy. Optics Letters. 1994; 19(11):780–782. DOI: 10.1364/ol.19.000780 [PubMed: 19844443]

[28]. Klar, Thomas A; Hell, Stefan W. Subdiffraction resolution in far-field fluorescence microscopy. Optics Letters. 1999; 24(14):954–956. DOI: 10.1364/ol.24.000954 [PubMed: 18073907]

[29]. Klar, Thomas A; Jakobs, Stefan; Dyba, Marcus; Egner, Alexander; Hell, Stefan W. Fluorescence microscopy with diffraction resolution barrier broken by stimulated emission. Proceedings of the National Academy of Sciences. 2000; 97(15):8206–8210. DOI: 10.1073/pnas.97.15.8206

[30]. Hell SW, Stelzer EHK. Properties of a 4Pi confocal fluorescence microscope. Optical Society of America. Journal A: Optics, Image Science, and Vision. 1992; 9:2159–2166. DOI: 10.1364/josaa.9.002159

[31]. Gustafsson MGL, Agard DA, Sedat JW. I5M: 3D widefield light microscopy with better than 100 nm axial resolution. Journal of Microscopy. 1999; 195:10–16. DOI: 10.1046/j.1365-2818.1999.00576.x [PubMed: 10444297]

[32]. Gustafsson MGL. Surpassing the lateral resolution limit by a factor of two using structured illumination microscopy. Journal of Microscopy. 2000; 198(2):82–87. DOI: 10.1046/j.1365-2818.2000.00710.x [PubMed: 10810003]

[33]. Gustafsson, Mats GL; Shao, Lin; Carlton, Peter M; Rachel, Wang CJ; Golubovskaya, Inna N; Zacheus, Cande W; Agard, David A; Sedat, John W. Three-dimensional resolution doubling in wide-field fluorescence microscopy by structured illumination. Biophysical Journal. 2008; 94(12):4957–4970. DOI: 10.1529/biophysj.107.120345 [PubMed: 18326650]

[34]. Gustafsson MGL. Nonlinear structured-illumination microscopy: Wide-field fluorescence imaging with theoretically unlimited resolution. Proceedings of the National Academy of Sciences. 2005; 102(37):13081–13086. DOI: 10.1073/pnas.0406877102

[35]. Heintzmann R, Jovin TM, Cremer C. Saturated patterned excitation microscopy – a concept for optical resolution improvement. Journal of the Optical Society of America. A, Optics, image science, and vision. 2002; 19(8):1599–1609. DOI: 10.1364/josaa.19.001599

[36]. Chen F, Tillberg PW, Boyden ES. Expansion microscopy. Science. 2015; 347(6221):543–548. DOI: 10.1126/science.1260088 [PubMed: 25592419]

[37]. Chang, Jae-Byum; Chen, Fei; Yoon, Young-Gyu; Jung, Erica E; Babcock, Hazen; Jeong, Seuk Kang; Asano, Shoh; Suk, Ho-Jun; Pak, Nikita; Tillber, Paul W; Wassie, Asmamaw T; , et al.

Iterative expansion microscopy. Nature Methods. 2017; 14:593–599. DOI: 10.1038/nmeth.4261 [PubMed: 28417997]

[38]. Truckenbrodt, Sven; Maidorn, Manuel; Crzan, Dagmar; Wildhagen, Hanna; Kabatas, Selda; Rizzoli, Silvio O. X10 expansion microscopy enables 25-nm resolution on conventional microscopes. EMBO Reports. 2018; 19(9):e45836.doi: 10.15252/embr.201845836 [PubMed: 29987134]

[39]. Truckenbrodt, Sven; Sommer, Christoph; Rizzoli, Silvio O; Danzl, Johann G. A practical guide to optimization in X10 expansion microscopy. Nature Protocols. 2019; doi: 10.1038/s41596-018-0117-3

[40]. Lakowicz, Joseph R. Principles of Fluorescence Spectroscopy. 3 edition. Springer Science + Business Media; 2006.

[41]. Sandell, Julia L; Zhu, Timothy C. A review of *in-vivo* optical properties of human tissues and its impact on PDT. Journal of Biophotonics. 2011; 4(11–12):773–787. DOI: 10.1002/jbio.201100062 [PubMed: 22167862]

[42]. Jacques, Steven L. Optical properties of biological tissues: a review. Physics in Medicine and Biology. 2013; 58:37–61. DOI: 10.1088/0031-9155/58/11/R37

[43]. Ntziachristos, Vasilis. Going deeper than microscopy: The optical imaging frontier in biology. Nature Methods. 2010; 7(8):603–614. DOI: 10.1038/nmeth.1483 [PubMed: 20676081]

[44]. Sharpe, James. Optical Projection Tomography. 2004; :209–228. DOI: 10.1146/annurev.bioeng.6.040803.140210

[45]. Hong, Guosong; Antaris, Alexander L; Dai, Hongjie. Near-infrared fluorophores for biomedical imaging. Nature Biomedical Engineering. 2017; 1(1):0010.doi: 10.1038/s41551-016-0010

[46]. Eggeling, C, Widengren, J, Rigler, R, Seidel, CAM. Photostability of fluorescent dyes for single-molecule spectroscopy: Mechanisms and experimental methods for estimating photobleaching in aqueous solutionApplied Fluorescence in Chemistry, Biology and Medicine. Springer Berlin Heidelberg; 1999. 193–240.

[47]. Leutenegger, Marcel; Eggeling, Christian; Hell, Stefan W. Analytical description of STED microscopy performance. Optics Express. 2010; 18(25):26417.doi: 10.1364/oe.18.026417 [PubMed: 21164992]

[48]. Tortarolo, Giorgio; Castello, Marco; Diaspro, Alberto; Koho, Sami; Vicidomini, Giuseppe. Evaluating image resolution in stimulated emission depletion microscopy. Optica. 2018; 5(1):32–35. DOI: 10.1364/OPTICA.5.000032

[49]. Laissue, P Philippe; Alghamdi, Rana A; Tomancak, Pavel; Reynaud, Emmanuel G; Shroff, Hari. Assessing phototoxicity in live fluorescence imaging. Nature Methods. 2017; 14(7):657–661. DOI: 10.1038/nmeth.4344 [PubMed: 28661494]

[50]. Wäldchen, Sina; Lehmann, Julian; Klein, Teresa; van de Linde, Sebastian; Sauer, Markus. Light-induced cell damage in live-cell super-resolution microscopy. Scientific Reports. 2015; 5(1)doi: 10.1038/srep15348

[51]. Kilian, Nicole; Goryaynov, Alexander; Lessard, Mark D; Hooker, Giles; Toomre, Derek; Rothman, James E; Bewersdorf, Joerg. Assessing photodamage in live-cell STED microscopy. Nature Methods. 2018; 15(10):755–756. DOI: 10.1038/s41592-018-0145-5 [PubMed: 30275592]

[52]. Danzl, Johann G; Sidenstein, Sven C; Gregor, Carola; Urban, Nicolai T; Ilgen, Peter; Jakobs, Stefan; Hell, Stefan W. Coordinate-targeted fluorescence nanoscopy with multiple off states. Nature Photonics. 2016; 10(2):122.doi: 10.1038/nphoton.2015.266

[53]. Eilers, Yvan; Ta, Haisen; Gwosch, Klaus C; Balzarotti, Francisco; Hell, Stefan W. MINFLUX monitors rapid molecular jumps with superior spatiotemporal resolution. Proceedings of the National Academy of Sciences. 2018; 115(24):6117–6122. DOI: 10.1073/pnas.1801672115

[54]. Gould, Travis J, Pellett, Patrina A, Bewersdorf, Joerg. STED Microscopy. Wiley-VCH; 2013.

[55]. Eggeling C, Willig KI, Sahl SJ, Hell SW. Lens-based fluorescence nanoscopy. Quarterly Reviews of Biophysics. 2015; 48(2):178–243. DOI: 10.1017/S0033583514000146 [PubMed: 25998828]

[56]. Hell, Stefan W; Sahl, Steffen J; Bates, Mark; Zhuang, Xiaowei; Heintzmann, Rainer; Booth, Martin J; Bewersdorf, Joerg; Shtengel, Gleb; Hess, Harald; Tinnefeld, Philip; Honigmann, Alf; , et al. The 2015 super-resolution microscopy roadmap. Journal of Physics D: Applied Physics. 2015; 48(44)doi: 10.1088/0022-3727/48/44/443001

[57]. Blom, Hans; Widengren, Jerker. Stimulated emission depletion microscopy. Chemical Reviews. 2017; 117(11):7377–7427. DOI: 10.1021/acs.chemrev.6b00653 [PubMed: 28262022]

[58]. Vicidomini, Giuseppe; Bianchini, Paolo; Diaspro, Alberto. STED super-resolved microscopy. Nature Methods. 2018; 15(3):173–182. DOI: 10.1038/nmeth.4593 [PubMed: 29377014]

[59]. Birk, Udo J. Super-Resolution Microscopy. Wiley VCH Verlag GmbH; 2017. ISBN 3527341331

[60]. Rittweger E, Rankin BR, Westphal V, Hell SW. Fluorescence depletion mechanisms in super-resolving STED microscopy. Chemical Physics Letters. 2007; 442(4-6):483–487. DOI: 10.1016/j.cplett.2007.06.017

[61]. Keller, Jan; Schönle, Andreas; Hell, Stefan W. Efficient fluorescence inhibition patterns for RESOLFT microscopy. Optics Express. 2007; 15(6):3361.doi: 10.1364/oe.15.003361 [PubMed: 19532577]

[62]. Moneron, Gael; Hell, Stefan W. Two-photon excitation STED microscopy. Optics Express. 2009; 17(17):14567–14573. DOI: 10.1364/oe.17.014567 [PubMed: 19687936]

[63]. Ding, Jun B; Takasaki, Kevin T; Sabatini, Bernardo L. Supraresolution imaging in brain slices using stimulated-emission depletion two-photon laser scanning microscopy. Neuron. 2009; 63:429–437. DOI: 10.1016/j.neuron.2009.07.011 [PubMed: 19709626]

[64]. Li Q, Wu SSH, Chou KC. Subdiffraction-limit two-photon fluorescence microscopy for GFP-tagged cell imaging. Biophysical Journal. 2009; 97(12):3224–3228. DOI: 10.1016/j.bpj.2009.09.038 [PubMed: 20006960]

[65]. Bianchini P, Harke B, Galiani S, Vicidomini G, Diaspro A. Single-wavelength two-photon excitation-stimulated emission depletion (SW2PE-STED) superresolution imaging. Proceedings of the National Academy of Sciences. 2012; 109(17):6390–6393. DOI: 10.1073/pnas.1119129109

[66]. Bethge, Philipp; Chéreau, Ronan; Avignone, Elena; Marsicano, Giovanni; Nägerl, Valentin U. Two-photon excitation STED microscopy in two colors in acute brain slices. Biophysical Journal. 2013; 104(4):778–785. DOI: 10.1016/j.bpj.2012.12.054 [PubMed: 23442956]

[67]. Dyba M, Hell SW. Focal spots of size λ/23 open up far-field florescence microscopy at 33 nm axial resolution. Physical Review Letters. 2002; 88(16):163901.doi: 10.1103/PhysRevLett.88.163901 [PubMed: 11955234]

[68]. Schmidt, Roman; Wurm, Christian A; Jakobs, Stefan; Engelhardt, Johann; Egner, Alexander; Hell, Stefan W. Spherical nanosized focal spot unravels the interior of cells. Nature Methods. 2008; 5(6):539–544. DOI: 10.1038/nmeth.1214 [PubMed: 18488034]

[69]. Hell, Stefan W. Toward fluorescence nanoscopy. Nature Biotechnology. 2003; 21(11):1347.doi: 10.1038/nbt895

[70]. Harke, Benjamin; Keller, Jan; Ullal, Chaitanya K; Westphal, Volker; Schönle, Andreas; Hell, Stefan W. Resolution scaling in STED microscopy. Optics Express. 2008; 16(6):4154–4162. DOI: 10.1364/oe.16.004154 [PubMed: 18542512]

[71]. Rittweger, Eva; Han, Kyu Young; Irvine, Scott E; Eggeling, Christian; Hell, Stefan W. STED microscopy reveals crystal colour centres with nanometric resolution. Nature Photonics. 2009; 3(3):144.doi: 10.1038/nphoton.2009.2

[72]. Schneider, Jale; Zahn, Jasmin; Maglione, Marta; Sigrist, Stephan J; Marquard, Jonas; Chojnacki, Jakub; Kräusslich, Hans-Georg; Sahl, Steffen J; Engelhardt, Johann; Hell, Stefan W. Ultrafast, temporally stochastic STED nanoscopy of millisecond dynamics. Nature Methods. 2015; 12(9):827–830. DOI: 10.1038/nmeth.3481 [PubMed: 26214129]

[73]. Nägerl, U Valentin; Willig, Katrin I; Hein, Birka; Hell, Stefan W; Bonhoeffer, Tobias. Live-cell imaging of dendritic spines by STED microscopy. Proceedings of the National Academy of Sciences. 2008; 105(48)doi: 10.1073/pnas.0810028105

[74]. Tønnesen, Jan; Inavalli, VVG Krishna; Nägerl, U Valentin. Super-resolution imaging of the extracellular space in living brain tissue. Cell. 2018; 172(5):1108–1121.e15. DOI: 10.1016/j.cell.2018.02.007 [PubMed: 29474910]

[75]. Eggeling C, Ringemann C, Medda R, Schwarzmann G, Sandhoff K, Polyakova S, Belov VN, Hein B, von Middendorff C, Schönle A, Hell SW. Direct observation of the nanoscale dynamics of membrane lipids in a living cell. Nature. 2009; 457:1159–1162. DOI: 10.1038/nature07596 [PubMed: 19098897]

[76]. Denk, Winfried; Strickler, James H; Webb, Watt W. Two-photon laser scanning fluorescence microscopy. Science. 1990; 248(4951):73–76. DOI: 10.1126/science.2321027 [PubMed: 2321027]

[77]. Göttfert, Fabian; Wurm, Christian A; Mueller, Veronika; Berning, Sebastian; Cordes, Volker C; Honigmann, Alf; Hell, Stefan W. Coaligned dual-channel STED nanoscopy and molecular diffusion analysis at 20 nm resolution. Biophysical Journal. 2013; 105(1):L01–L03. DOI: 10.1016/j.bpj.2013.05.029 [PubMed: 23823248]

[78]. Willig KI, Harke B, Medda R, Hell SW. STED microscopy with continuous wave beams. Nature Methods. 2007; 4(11):915–918. DOI: 10.1038/nmeth1108 [PubMed: 17952088]

[79]. Moneron, Gael; Medda, Rebecca; Hein, Birka; Giske, Arnold; Westphal, Volker; Hell, Stefan W. Fast STED microscopy with continuous wave fiber lasers. Optics Express. 2010; 18(2):1302–1309. DOI: 10.1364/oe.18.001302 [PubMed: 20173956]

[80]. Vicidomini, Giuseppe; Moneron, Gael; Han, Kyu Y; Westphal, Volker; Ta, Haisen; Reuss, Matthias; Engelhardt, Johann; Eggeling, Christian; Hell, Stefan W. Sharper low-power STED nanoscopy by time gating. Nature Methods. 2011; 8(7):571.doi: 10.1038/nmeth.1624 [PubMed: 21642963]

[81]. Moffitt, Jeffrey R; Osseforth, Christian; Michaelis, Jens. Time-gating improves the spatial resolution of STED microscopy. Optics Express. 2011; 19(5):4242–4254. DOI: 10.1364/oe.19.004242 [PubMed: 21369254]

[82]. Vicidomini, Giuseppe; Schönle, Andreas; Ta, Haisen; Han, Kyu Young; Moneron, Gael; Eggeling, Christian; Hell, Stefan W. STED nanoscopy with time-gated detection: Theoretical and experimental aspects. PLoS ONE. 2013; 8(1):e54421.doi: 10.1371/journal.pone.0054421 [PubMed: 23349884]

[83]. Tønnesen, Jan; Nadrigny, Fabien; Willig, Katrin I; Wedlich-Söldner, Roland; Nägerl, U Valentin. Two-color STED microscopy of living synapses using a single laser-beam pair. Biophysical Journal. 2011; 101(10):2545–2552. DOI: 10.1016/j.bpj.2011.10.011 [PubMed: 22098754]

[84]. Görlitz, Frederik; Hoyer, Patrick; Falk, Henning; Kastrup, Lars; Engelhardt, Johann; Hell, Stefan W. A STED microscope designed for routine biomedical applications. Progress In Electromagnetics Research. 2014; 147:57–68. DOI: 10.2528/pier14042708

[85]. Sidenstein, Sven C; DEste, Elisa; Böhm, Marvin J; Danzl, Johann G; Belov, Vladimir N; Hell, Stefan W. Multicolour multilevel sted nanoscopy of actin/spectrin organization at synapses. Scientific Reports. 2016; 6doi: 10.1038/srep26725

[86]. Winter, Franziska R; Loidolt, Maria; Westphal, Volker; Butkevich, Alexey N; Gregor, Carola; Sahl, Steffen J; Hell, Stefan W. Multicolour nanoscopy of fixed and living cells with a single STED beam and hyperspectral detection. Scientific Reports. 2017; doi: 10.1038/srep46492

[87]. Hell SW, Jakobs S, Kastrup L. Imaging and writing at the nanoscale with focused visible light through saturable optical transitions. Applied Physics A. 2003; 77(7):859–860. DOI: 10.1007/s00339-003-2292-4

[88]. Hofmann, Michael; Eggeling, Christian; Jakobs, Stefan; Hell, Stefan W. Breaking the diffraction barrier in fluorescence microscopy at low light intensities by using reversibly photoswitchable proteins. Proceedings of the National Academy of Sciences. 2005; 102(49):17565–17569. DOI: 10.1073/pnas.0506010102

[89]. Andresen M, Wahl MC, Stiel AC, Gräter F, Schäfer LV, Trowitzsch S, Weber G, Eggeling C, Grubmüller H, Hell SW, Jakobs S. Structure and mechanism of the reversible photoswitch of a fluorescent protein. Proceedings of the National Academy of Sciences. 2005; 102:13070–13074. DOI: 10.1073/pnas.0502772102

[90]. Grotjohann T, Testa I, Leutenegger M, Bock H, Urban NT, Lavoie-Cardinal F, Willig KI, Eggeling C, Jakobs S, Hell SW. Diffraction-unlimited all-optical imaging and writing with a photochromic GFP. Nature. 2011; 478(7368):204–208. DOI: 10.1038/nature10497 [PubMed: 21909116]

[91]. Grotjohann, Tim; Testa, Ilaria; Reuss, Matthias; Brakemann, Tanja; Eggeling, Christian; Hell, Stefan W; Jakobs, Stefan. rsEGFP2 enables fast RESOLFT nanoscopy of living cells. eLife. 2012; 1doi: 10.7554/elife.00248

[92]. Brakemann T, Stiel AC, Weber G, Andresen M, Testa I, Grotjohann T, Leutenegger M, Plessmann U, Urlaub H, Eggeling C, Wahl MC, et al. A reversibly photoswitchable GFP-like protein with fluorescence excitation decoupled from switching. Nature Biotechnology. 2011; 29(10):942–947. DOI: 10.1038/nbt.1952

[93]. Pennacchietti, Francesca; Serebrovskaya, Ekaterina O; Faro, Aline R; Shemyakina, Irina I; Bozhanova, Nina G; Kotlobay, Alexey A; Gurskaya, Nadya G; Bodén, Andreas; Dreier, Jes; Chudakov, Dmitry M; Lukyanov, Konstantin A; , et al. Fast reversibly photoswitching red fluorescent proteins for live-cell RESOLFT nanoscopy. Nature Methods. 2018; 15(8):601–604. DOI: 10.1038/s41592-018-0052-9 [PubMed: 29988095]

[94]. Kwon, Jiwoong; Hwang, Jihee; Park, Jaewan; Han, Gi Rim; Han, Kyu Young; Kim, Seong Keun. RESOLFT nanoscopy with photoswitchable organic fluorophores. Scientific Reports. 2015; 5(1)doi: 10.1038/srep17804

[95]. Roubinet, Benoît; Bossi, Mariano L; Alt, Philipp; Leutenegger, Marcel; Shojaei, Heydar; Schnorrenberg, Sebastian; Nizamov, Shamil; Irie, Masahiro; Belov, Vladimir N; Hell, Stefan W. Carboxylated photoswitchable diarylethenes for biolabeling and super-resolution RESOLFT microscopy. Angewandte Chemie International Edition. 2016; 55(49):15429–15433. DOI: 10.1002/anie.201607940 [PubMed: 27767250]

[96]. Shao, Baihao; Baroncini, Massimo; Qian, Hai; Bussotti, Laura; Di Donato, Mariangela; Credi, Alberto; Aprahamian, Ivan. Solution and solid-state emission toggling of a photochromic hydrazone. Journal of the American Chemical Society. 2018; 140(39):12323–12327. DOI: 10.1021/jacs.8b07108 [PubMed: 30251843]

[97]. Xiong, Yaoyao; Jentzsch, Andreas Vargas; Osterrieth, Johannes WM; Sezgin, Erdinc; Sazanovich, Igor V; Reglinski, Katharina; Galiani, Silvia; Parker, Anthony W; Eggeling, Christian; Anderson, Harry L. Spironaphthoxazine switchable dyes for biological imaging. Chemical Science. 2018; 9(11):3029–3040. DOI: 10.1039/c8sc00130h [PubMed: 29732087]

[98]. Vicidomini, Giuseppe; Moneron, Gael; Eggeling, Christian; Rittweger, Eva; Hell, Stefan W. STED with wavelengths closer to the emission maximum. Optics Express. 2012; 20(5):5225.doi: 10.1364/oe.20.005225 [PubMed: 22418329]

[99]. Hotta, Jun-ichi; Fron, Eduard; Dedecker, Peter; Janssen, Kris PF; Li, Chen; Müller, Klaus; Harke, Benjamin; Bückers, Johanna; Hell, Stefan W; Hofkens, Johan. Spectroscopic rationale for efficient stimulated-emission depletion microscopy fluorophores. JACS. 2010; 132:5021–5023. DOI: 10.1021/ja100079w

[100]. Muyldermans, Serge. Nanobodies: Natural single-domain antibodies. Annual Review of Biochemistry. 2013; 82(1):775–797. DOI: 10.1146/annurev-biochem-063011-092449

[101]. Willig, Katrin I; Kellner, Robert R; Medda, Rebecca; Hein, Birka; Jakobs, Stefan; Hell, Stefan W. Nanoscale resolution in GFP-based microscopy. Nature Methods. 2006; 3(9):721–723. DOI: 10.1038/nmeth922 [PubMed: 16896340]

[102]. Lukinavičius G, Umezawa K, Olivier N, Honigmann A, Yang G, Plass T, Mueller V, Reymond L, Corrêa IR Jr, Luo ZG, Schultz C, et al. A near-infrared fluorophore for live-cell super-resolution microscopy of cellular proteins. Nature Chemistry. 2013; 5(2):132–139. DOI: 10.1038/nchem.1546

[103]. Grimm, Jonathan B; English, Brian P; Chen, Jiji; Slaughter, Joel P; Zhang, Zhengjian; Revyakin, Andrey; Patel, Ronak; Macklin, John J; Normanno, Davide; Singer, Robert H; Lionnet, Timothée; , et al. A general method to improve fluorophores for live-cell and single-molecule microscopy. Nature Methods. 2015; 12(3):244–250. DOI: 10.1038/nmeth.3256 [PubMed: 25599551]

[104]. Bottanelli, Francesca; Kromann, Emil B; Allgeyer, Edward S; Erdmann, Roman S; Baguley, Stephanie Wood; Sirinakis, George; Schepartz, Alanna; Baddeley, David; Toomre, Derek K; Rothman, James E; Bewersdorf, Joerg. Two-colour live-cell nanoscale imaging of intracellular targets. Nature Communications. 2016; 7(1)doi: 10.1038/ncomms10778

[105]. Butkevich, Alexey N; Mitronova, Gyuzel Yu; Sidenstein, Sven C; Klocke, Jessica L; Kamin, Dirk; Meineke, Dirk NH; D'Este, Elisa; Kraemer, Philip-Tobias; Danzl, Johann G; Belov, Vladimir N; Hell, Stefan W. Fluorescent rhodamines and fluorogenic carbopyronines for super-resolution STED microscopy in living cells. Angewandte Chemie International Edition. 2016; 55(10):3290–3294. DOI: 10.1002/anie.201511018 [PubMed: 26844929]

[106]. Grimm, Jonathan B; Muthusamy, Anand K; Liang, Yajie; Brown, Timothy A; Lemon, William C; Patel, Ronak; Lu, Rongwen; Macklin, John J; Keller, Philipp J; Ji, Na; Lavis, Luke D. A general method to fine-tune fluorophores for live-cell and in vivo imaging. Nature Methods. 2017; 14(10):987–994. DOI: 10.1038/nmeth.4403 [PubMed: 28869757]

[107]. Mollwitz, Birgit; Brunk, Elizabeth; Schmitt, Simone; Pojer, Florence; Bannwarth, Michael; Schiltz, Marc; Rothlisberger, Ursula; Johnsson, Kai. Directed evolution of the suicide protein o^6-alkylguanine-DNA alkyltransferase for increased reactivity results in an alkylated protein with exceptional stability. Biochemistry. 2012; 51(5):986–994. DOI: 10.1021/bi2016537 [PubMed: 22280500]

[108]. Los, Georgyi V; Encell, Lance P; McDougall, Mark G; Hartzell, Danette D; Karassina, Natasha; Zimprich, Chad; Wood, Monika G; Learish, Randy; Ohana, Rachel Friedman; Urh, Marjeta; Simpson, Dan; , et al. HaloTag: A novel protein labeling technology for cell imaging and protein analysis. ACS Chemical Biology. 2008; 3(6):373–382. DOI: 10.1021/cb800025k [PubMed: 18533659]

[109]. Rostovtsev, Vsevolod V; Green, Luke G; Fokin, Valery V; Sharpless, K Barry. A stepwise huisgen cycloaddition process: Copper(I)-catalyzed regioselective “ligation” of azides and terminal alkynes. Angewandte Chemie International Edition. 2002; 41(14):2596–2599. DOI: 10.1002/1521-3773(20020715)41:14<2596::aidanie2596>3.0.co;2-4 [PubMed: 12203546]

[110]. Crivat, Georgeta; Taraska, Justin W. Imaging proteins inside cells with fluorescent tags. Trends in Biotechnology. 2012; 30(1):8–16. DOI: 10.1016/j.tibtech.2011.08.002 [PubMed: 21924508]

[111]. Ries, Jonas; Kaplan, Charlotte; Platonova, Evgenia; Eghlidi, Hadi; Ewers, Helge. A simple, versatile method for GFP-based super-resolution microscopy via nanobodies. Nature Methods. 2012; 9(6):582–584. DOI: 10.1038/nmeth.1991 [PubMed: 22543348]

[112]. Kasper, Robert; Harke, Benjamin; Forthmann, Carsten; Tinnefeld, Philip; Hell, Stefan W; Sauer, Markus. Single-molecule STED microscopy with photostable organic fluorophores. Small. 2010; 6(13):1379–1384. DOI: 10.1002/smll.201000203 [PubMed: 20521266]

[113]. Liphardt, Bodo; Liphardt, Bernd; Lüttke, W. Laser dyes with intramolecular triplet quenching. Optics Communications. 1981; 38:207–210. DOI: 10.1016/0030-4018(81)90325-4

[114]. Altman, Roger B; Terry, Daniel S; Zhou, Zhou; Zheng, Qinsi; Geggier, Peter; Kolster, Rachel A; Zhao, Yongfang; Javitch, Jonathan A; Warren, J David; Blanchard, Scott C. Cyanine fluorophore derivatives with enhanced photostability. Nature Methods. 2011; 9(1):68–71. DOI: 10.1038/nmeth.1774 [PubMed: 22081126]

[115]. van der Velde, Jasper HM; Ploetz, Evelyn; Hiermaier, Matthias; Oelerich, Jens; de Vries, Jan Willem; Roelfes, Gerard; Cordes, Thorben. Mechanism of intramolecular photostabilization in self-healing cyanine fluorophores. ChemPhysChem. 2013; 14(18):4084–4093. DOI: 10.1002/cphc.201300785 [PubMed: 24302532]

[116]. Zheng, Qinsi; Jockusch, Steffen; Rodríguez-Calero, Gabriel G; Zhou, Zhou; Zhao, Hong; Altman Roger, B; Abruña, Héctor D; Blanchard Scott, C. Intramolecular triplet energy transfer is a general approach to improve organic fluorophore photostability. Photochemical & Photobiological Sciences. 2016; 15(2):196–203. DOI: 10.1039/c5pp00400d [PubMed: 26700693]

[117]. van der Velde, Jasper HM; Oelerich, Jens; Huang, Jingyi; Smit, Jochem H; Jazi, Atieh Aminian; Galiani, Silvia; Kolmakov, Kirill; Gouridis, Giorgos; Eggeling, Christian; Herrmann, Andreas; Roelfes, Gerard; Cordes, Thorben. A simple and versatile design concept for fluorophore derivatives with intramolecular photostabilization. Nature Communications. 2016; 7(1)doi: 10.1038/ncomms10144

[118]. van der Velde, Jasper HM; Smit, Jochem H; Hebisch, Elke; Punter, Michiel; Cordes, Thorben. Self-healing dyes for super-resolution fluorescence microscopy. Journal of Physics D: Applied Physics. 2018; 52(3):034001.doi: 10.1088/1361-6463/aae752

[119]. Riedl, Julia; Crevenna, Alvaro H; Kessenbrock, Kai; Yu, Jerry Haochen; Neukirchen, Dorothee; Bista, Michal; Bradke, Frank; Jenne, Dieter; Holak, Tad A; Werb, Zena; Sixt, Michael; Wedlich-Soldner, Roland. Lifeact: a versatile marker to visualize F-actin. Nature Methods. 2008; 5(7):605–607. DOI: 10.1038/nmeth.1220 [PubMed: 18536722]

[120]. Urban, Nicolai T; Willig, Katrin I; Hell, Stefan W; Nägerl, U Valentin. STED nanoscopy of actin dynamics in synapses deep inside living brain slices. Biophysical Journal. 2011; 101(5):1277–1284. DOI: 10.1016/j.bpj.2011.07.027 [PubMed: 21889466]

[121]. Spahn, Christoph; Grimm, Jonathan B; Lavis, Luke D; Lampe, Marko; Heilemann, Mike. Whole-cell, 3D, and multicolor STED imaging with exchangeable fluorophores. Nano Letters. 2018; 19(1):500–505. DOI: 10.1021/acs.nanolett.8b04385 [PubMed: 30525682]

[122]. Jungmann, Ralf; Avendaño, Maier S; Woehrstein, Johannes B; Dai, Mingjie; Shih, William M; Yin, Peng. Multiplexed 3d cellular super-resolution imaging with DNA-PAINT and exchange-PAINT. Nature Methods. 2014; 11(3):313–318. DOI: 10.1038/nmeth.2835 [PubMed: 24487583]

[123]. Beater, Susanne; Holzmeister, Phil; Lalkens, Birka; Tinnefeld, Philip. Simple and aberration-free 4color-STED - multiplexing by transient binding. Optics Express. 2015; 23(7):8630.doi: 10.1364/oe.23.008630 [PubMed: 25968701]

[124]. Schueder, Florian; Strauss, Maximilian T; Hoerl, David; Schnitzbauer, Joerg; Schlichthaerle, Thomas; Strauss, Sebastian; Yin, Peng; Harz, Hartmann; Leonhardt, Heinrich; Jungmann, Ralf. Universal super-resolution multiplexing by DNA exchange. Angewandte Chemie International Edition. 2017; 56(14):4052–4055. DOI: 10.1002/anie.201611729 [PubMed: 28256790]

[125]. Wang, Yu; Woehrstein, Johannes B; Donoghue, Noah; Dai, Mingjie; Avendaño, Maier S; Schackmann, Ron CJ; Zoeller, Jason J; Wang, Shan Shan H; Tillberg, Paul W; Park, Demian; Lapan, Sylvain W; , et al. Rapid sequential in situ multiplexing with DNA exchange imaging in neuronal cells and tissues. Nano Letters. 2017; 17(10):6131–6139. DOI: 10.1021/acs.nanolett.7b02716 [PubMed: 28933153]

[126]. Donnert, Gerald; Eggeling, Christian; Hell, Stefan W. Major signal increase in fluorescence microscopy through dark-state relaxation. Nature Methods. 2007; 4(1):81.doi: 10.1038/nmeth986 [PubMed: 17179937]

[127]. Donnert, Gerald; Keller, Jan; Medda, Rebecca; Alexandra, Andrei M; Rizzoli, Silvio O; Lührmann, Reinhard; Jahn, Reinhard; Eggeling, Christian; Hell, Stefan W. Macromolecular-scale resolution in biological fluorescence microscopy. Proceedings of the National Academy of Sciences. 2006; 103(31):11440–11445. DOI: 10.1073/pnas.0604965103

[128]. Westphal, Volker; Lauterbach, Marcel A; Di Nicola, Angelo; Hell, Stefan W. Dynamic far-field fluorescence nanoscopy. New Journal of Physics. 2007; 9(12):435.doi: 10.1088/1367-2630/9/12/435

[129]. Chen, Xiaowei; Leischner, Ulrich; Varga, Zsuzsanna; Jia, Hongbo; Deca, Diana; Rochefort, Nathalie L; Konnerth, Arthur. LOTOS-based two-photon calcium imaging of dendritic spines *in vivo*. Nature Protocols. 2012; 7(10):1818–1829. DOI: 10.1038/nprot.2012.106 [PubMed: 22976353]

[130]. Staudt, Thorsten; Engler, Andreas; Rittweger, Eva; Harke, Benjamin; Engelhardt, Johann; Hell, Stefan W. Far-field optical nanoscopy with reduced number of state transition cycles. Optics Express. 2011; 19(6):5644–5657. DOI: 10.1364/oe.19.005644 [PubMed: 21445205]

[131]. Hoebe RA, Van Oven CH, Gadella TWJ, Dhonukshe PB, Van Noorden CJF, Manders EMM. Controlled light-exposure microscopy reduces photobleaching and phototoxicity in fluorescence live-cell imaging. Nature Biotechnology. 2007; 25(2):249–253. DOI: 10.1038/nbt1278

[132]. Dreier, Jes; Castello, Marco; Coceano, Giovanna; Cáceres, Rodrigo; Plastino, Julie; Vicidomini, Giuseppe; Testa, Ilaria. Smart scanning for low-illumination and fast RESOLFT nanoscopy in vivo. Nature Communications. 2019; 10(1)doi: 10.1038/s41467-019-08442-4

[133]. Heine, Jörn; Reuss, Matthias; Harke, Benjamin; D'Este, Elisa; Sahl, Steffen J; Hell, Stefan W. Adaptive-illumination STED nanoscopy. Proceedings of the National Academy of Sciences. 2017; 114(37):9797–9802. DOI: 10.1073/pnas.1708304114

[134]. Göttfert, Fabian; Pleiner, Tino; Heine, Jörn; Westphal, Volker; Görlich, Dirk; Sahl, Steffen J; Hell, Stefan W. Strong signal increase in STED fluorescence microscopy by imaging regions of subdiffraction extent. Proceedings of the National Academy of Sciences. 2017; 114(9):2125–2130. DOI: 10.1073/pnas.1621495114

[135]. Chmyrov, Andriy; Keller, Jan; Grotjohann, Tim; Ratz, Michael; d'Este, Elisa; Jakobs, Stefan; Eggeling, Christian; Hell, Stefan W. Nanoscopy with more than 100,000 'doughnuts'. Nature Methods. 2013; 10(8):737–740. DOI: 10.1038/nmeth.2556 [PubMed: 23832150]

[136]. Antonello, Jacopo; Burke, Daniel; Booth, Martin J. Aberrations in stimulated emission depletion (STED) microscopy. Optics Communications. 2017; 404:203–209. DOI: 10.1016/j.optcom.2017.06.037 [PubMed: 29861506]

[137]. Li, Yanghui; Zhou, Hui; Liu, Xiaoyu; Li, Yuxue; Wang, Le. Effects of aberrations on effective point spread function in STED microscopy. Applied Optics. 2018; 57(15):4164.doi: 10.1364/ao.57.004164 [PubMed: 29791391]

[138]. Antonello, Jacopo; Kromann, Emil B; Burke, Daniel; Bewersdorf, Joerg; Booth, Martin J. Coma aberrations in combined two- and three-dimensional STED nanoscopy. Optics Letters. 2016; 41(15):3631.doi: 10.1364/ol.41.003631 [PubMed: 27472636]

[139]. Berning S, Willig KI, Steffens H, Dibaj P, Hell SW. Nanoscopy in a living mouse brain. Science. 2012; 335(6068):551–551. DOI: 10.1126/science.1215369 [PubMed: 22301313]

[140]. Chéreau, Ronan; Tønnesen, Jan; Nägerl, U Valentin. STED microscopy for nanoscale imaging in living brain slices. Methods. 2015; 88:57–66. DOI: 10.1016/j.ymeth.2015.06.006 [PubMed: 26070997]

[141]. Booth, Martin J. Adaptive optical microscopy: the ongoing quest for a perfect image. Light: Science & Applications. 2014; 3(4):e165.doi: 10.1038/lsa.2014.46

[142]. Lenz, Martin O; Sinclair, Hugo G; Savell, Alexander; Clegg, James H; Brown, Alice CN; Davis, Daniel M; Dunsby, Chris; Neil, Mark AA; French, Paul MW. 3-D stimulated emission depletion microscopy with programmable aberration correction. Journal of Biophotonics. 2013; 7(1–2):29–36. DOI: 10.1002/jbio.201300041 [PubMed: 23788459]

[143]. Gould, Travis J; Kromann, Emil B; Burke, Daniel; Booth, Martin J; Bewersdorf, Joerg. Auto-aligning stimulated emission depletion microscope using adaptive optics. Optics Letters. 2013; 38(11):1860–1862. DOI: 10.1364/ol.38.001860 [PubMed: 23722769]

[144]. Gould, Travis J; Burke, Daniel; Bewersdorf, Joerg; Booth, Martin J. Adaptive optics enables 3D STED microscopy in aberrating specimens. Optics Express. 2012; 20(19):20998–21009. DOI: 10.1364/oe.20.020998 [PubMed: 23037223]

[145]. Patton, Brian R; Burke, Daniel; Owald, David; Gould, Travis J; Bewersdorf, Joerg; Booth, Martin J. Three-dimensional STED microscopy of aberrating tissue using dual adaptive optics. Optics Express. 2016; 24(8):8862.doi: 10.1364/oe.24.008862 [PubMed: 27137319]

[146]. Görlitz, Frederik; Guldbrand, Stina; Runcorn, Timothy H; Murray, Robert T; Jaso-Tamame, Angel L; Sinclair, Hugo G; Martinez-Perez, Enrique; Taylor, James R; Neil, Mark AA; Dunsby, Christopher; French, Paul MW. easySLM-STED: Stimulated emission depletion microscopy with aberration correction, extended field of view and multiple beam scanning. Journal of Biophotonics. 2018; 11(11):e201800087.doi: 10.1002/jbio.201800087 [PubMed: 29978591]

[147]. Bingen, Pit; Reuss, Matthias; Engelhardt, Johann; Hell, Stefan W. Parallelized STED fluorescence nanoscopy. Optics Express. 2011; 19(24):23716–23726. DOI: 10.1364/oe.19.023716 [PubMed: 22109398]

[148]. Yang, Bin; Przybilla, Frédéric; Mestre, Michael; Trebbia, Jean-Baptiste; Lounis, Brahim. Large parallelization of STED nanoscopy using optical lattices. Optics Express. 2014; 22(5):5581–5589. DOI: 10.1364/oe.22.005581 [PubMed: 24663899]

[149]. Bergermann, Fabian; Alber, Lucas; Sahl, Steffen J; Engelhardt, Johann; Hell, Stefan W. 2000-fold parallelized dual-color STED fluorescence nanoscopy. Optics Express. 2015; 23(1):211.doi: 10.1364/oe.23.000211 [PubMed: 25835668]

[150]. Chmyrov, Andriy; Leutenegger, Marcel; Grotjohann, Tim; Schönle, Andreas; Keller-Findeisen, Jan; Kastrup, Lars; Jakobs, Stefan; Donnert, Gerald; Sahl, Steffen J; Hell, Stefan W. Achromatic light patterning and improved image reconstruction for parallelized RESOLFT nanoscopy. Scientific Reports. 2017; 7:44619.doi: 10.1038/srep44619 [PubMed: 28317930]

[151]. Yang, Bin; Przybilla, Frédéric; Mestre, Michael; Trebbia, Jean-Baptiste; Lounis, Brahim. Using optical lattice for STED parallelizationNanoimaging and Nanospectroscopy II. Verma, Prabhat; Egner, Alexander, editors. SPIE; 2014.

[152]. Yang B, Fang C-Y, Chang H-C, Treussart F, Trebbia J-B, Lounis B. Polarization effects in lattice-STED microscopy. Faraday Discuss. 2015; 184:37–49. DOI: 10.1039/c5fd00092k [PubMed: 26407019]

[153]. Masullo, Luciano A; Bodén, Andreas; Pennacchietti, Francesca; Coceano, Giovanna; Ratz, Michael; Testa, Ilaria. Enhanced photon collection enables four dimensional fluorescence nanoscopy of living systems. Nature Communications. 2018; 9(1)doi: 10.1038/s41467-018-05799-w

[154]. Xue, Yi; So, Peter TC. Three-dimensional super-resolution high-throughput imaging by structured illumination STED microscopy. Optics Express. 2018; 26(16):20920.doi: 10.1364/oe.26.020920 [PubMed: 30119399]

[155]. Huisken, Jan; Swoger, Jim; Del Bene, Filippo; Wittbrodt, Joachim; Stelzer, Ernst HK. Optical sectioning deep inside live embryos by selective plane illumination microscopy. Science. 2004; 305:1007–1009. DOI: 10.1126/science.1100035 [PubMed: 15310904]

[156]. Keller, Philipp J; Schmidt, Annette D; Wittbrodt, Joachim; Stelzer, Ernst HK. Reconstruction of zebrafish early embryonic development by scanned light sheet microscopy. Science. 2008; 322:1065–1069. DOI: 10.1126/science.1162493 [PubMed: 18845710]

[157]. Chen, Bi-Chang; Legant, Wesley R; Wang, Kai; Shao, Lin; Milkie, Daniel E; Davidson, Michael W; Janetopoulos, Chris; Wu, Xufeng S; Hammer, John A; Liu, Zhe; English, Brian P; , et al. Lattice light-sheet microscopy: Imaging molecules to embryos at high spatiotemporal resolution. Science. 2014; 346(6208):1257998.doi: 10.1126/science.1257998 [PubMed: 25342811]

[158]. Friedrich, Mike; Gan, Qiang; Ermolayev, Vladimir; Harms, Gregory S. STED-SPIM: Stimulated emission depletion improves sheet illumination microscopy resolution. Biophysical Journal. 2011; 100:43–45. DOI: 10.1016/j.bpj.2010.12.3748

[159]. Friedrich, Mike; Harms, Gregory S. Axial resolution beyond the diffraction limit of a sheet illumination microscope with stimulated emission depletion. Journal of Biomedical Optics. 2015; 20(10):106006.doi: 10.1117/1.jbo.20.10.106006 [PubMed: 26469565]

[160]. Hoyer, Patrick; Gustavo, de Medeiros; Balázs, Bálint; Norlin, Nils; Besir, Christina; Hanne, Janina; Kräusslich, Hans-Georg; Engelhardt, Johann; Sahl, Steffen J; Hell, Lars. Breaking the diffraction limit of light-sheet fluorescence microscopy by RESOLFT. Proceedings of the National Academy of Sciences. 2016; 113(13):3442–3446. DOI: 10.1073/pnas.1522292113

[161]. Fahrbach, Florian O; Rohrbach, Alexander. A line scanned light-sheet microscope with phase shaped self-reconstructing beams. Optics Express. 2010; 18(23):24229–24244. DOI: 10.1364/oe.18.024229 [PubMed: 21164769]

[162]. Planchon, Thomas A; Gao, Liang; Milkie, Daniel E; Davidson, Michael W; Galbraith, James A; Galbraith, Catherine G; Betzig, Eric. Rapid three-dimensional isotropic imaging of living cells using Bessel beam plane illumination. Nature Methods. 2011; 8(5):417–423. DOI: 10.1038/nmeth.1586 [PubMed: 21378978]

[163]. Fahrbach, Florian O; Gurchenkov, Vasily; Alessandri, Kevin; Nassoy, Pierre; Rohrbach, Alexander. Self-reconstructing sectioned Bessel beams offer submicron optical sectioning for large fields of view in light-sheet microscopy. Optics Express. 2013; 21(9):11425–11440. DOI: 10.1364/oe.21.011425 [PubMed: 23669999]

[164]. Fahrbach, Florian O; Gurchenkov, Vasily; Alessandri, Kevin; Nassoy, Pierre; Rohrbach, Alexander. Light-sheet microscopy in thick media using scanned Bessel beams and two-photon fluorescence excitation. Optics Express. 2013; 21(11):13824–13839. DOI: 10.1364/oe.21.013824 [PubMed: 23736637]

[165]. Zhang P, Goodwin PM, Werner JH. Fast, super resolution imaging via Bessel-beam stimulated emission depletion microscopy. Optics Express. 2014; 22(10):12398.doi: 10.1364/oe.22.012398 [PubMed: 24921358]

[166]. Gohn-Kreuz, Cristian; Rohrbach, Alexander. Light-sheet generation in inhomogeneous media using self-reconstructing beams and the STED-principle. Optics Express. 2016; 24(6):5855.doi: 10.1364/oe.24.005855 [PubMed: 27136782]

[167]. Gohn-Kreuz, Cristian; Rohrbach, Alexander. Light needles in scattering media using self-reconstructing beams and the STED principle. Optica. 2017; 4(9):1134.doi: 10.1364/optica.4.001134

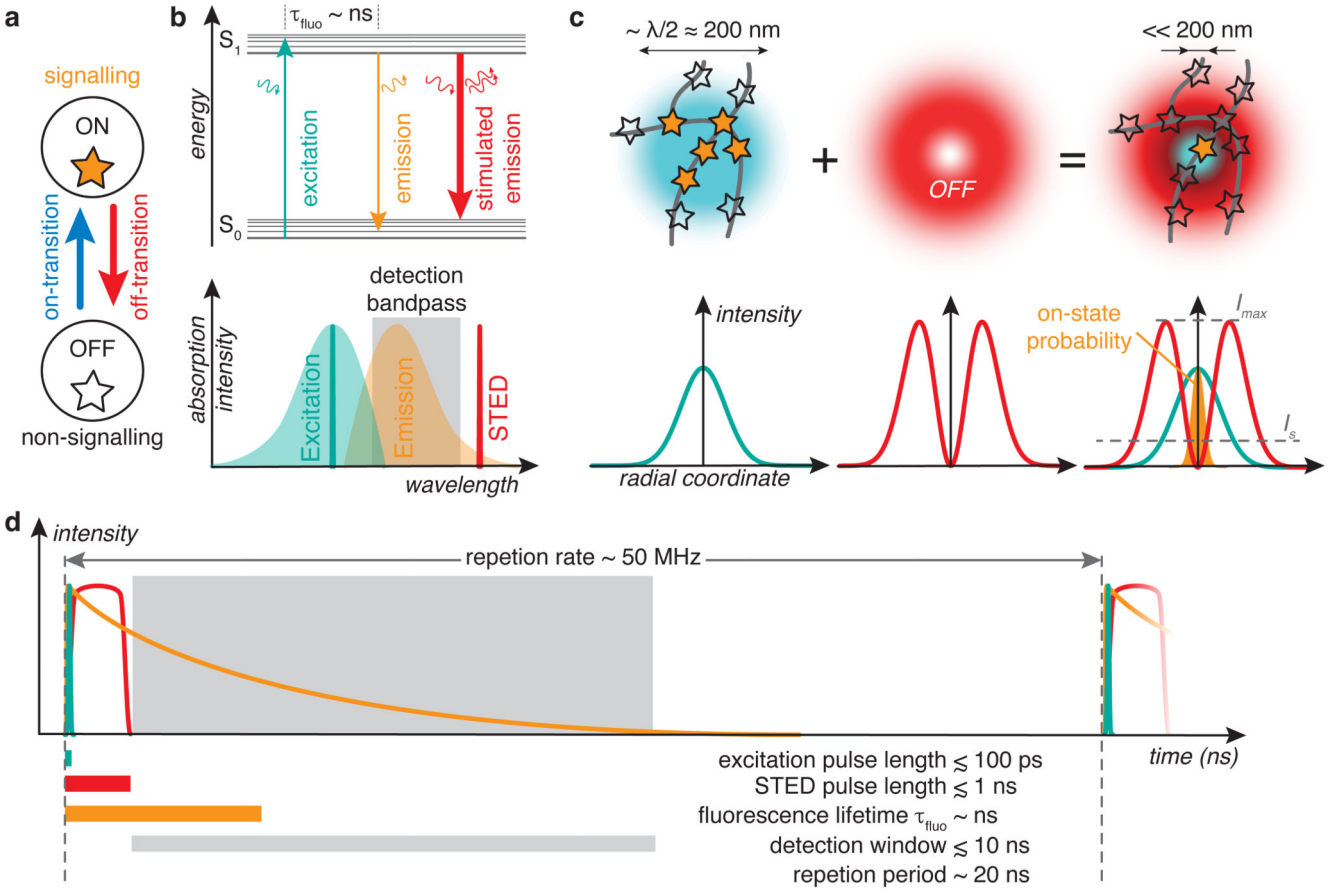

Figure 1.

STED nanoscopy. **a** Schematic of molecular states for nanoscopy. **b** *Top:* Energy diagram. S_0, singlet ground state; S_1, first excited state; τ_{fluo}, fluorescence lifetime. Curved arrows: photons. *Bottom:* Excitation and emission spectra of typical fluorophore with wavelengths for excitation and STED (vertical lines) and detection window. **c** *Left:* In conventional laser-scanning microscopy, all fluorophores within a diffraction-limited laser focus are excited simultaneously (orange stars) and are hence indistinguishable. *Middle and right:* In STED nanoscopy, a light pattern superimposed with the excitation focus transiently silences fluorophores (black stars) except for those located at an intensity zero, thus making fluorophores distinguishable on sub-diffraction length scales. I_S, saturation intensity; I_{max}, maximum STED intensity. **d** Timing in STED nanoscopy. The scale is zoomed into an individual excitation (cyan) and STED (red) pulse pair. Fluorescence signal time course (orange) is indicated for the location of the STED light intensity zero. Signal integration time is typically (tens of) µs at each scan position. Colour code applies to all figures.

Europe PMC Funders Author Manuscripts

Europe PMC Funders Author Manuscripts

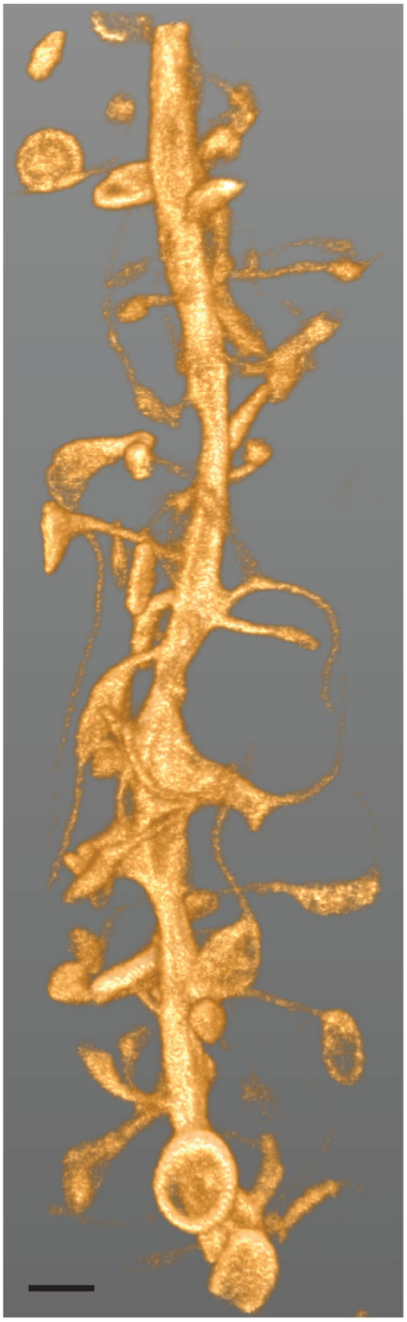

Figure 2.

Diffraction-unlimited imaging of a portion of a neuronal dendrite in living brain tissue with resolution increase in *xy*- and *z*-directions. Volume rendering of a 3D-image stack comprising 56 *z*-slices recorded with protected STED. Actin is labelled by an intracellularly expressed nanobody fused to a reversibly photoswitchable fluorescent protein (rsEGFP2) after viral delivery in an organotypic hippocampal brain slice. A multitude of dendritic spines, the postsynaptic compartments of excitatory synapses, emanate from the dendritic shaft. Spine necks exhibit sub-diffraction widths. In some spine heads, peculiar ring-like

actin structures can be discerned. Scale bar: 1 μm. Reproduced with permission from Ref. Danzl et al.[52].

Europe PMC Funders Author Manuscripts

Europe PMC Funders Author Manuscripts

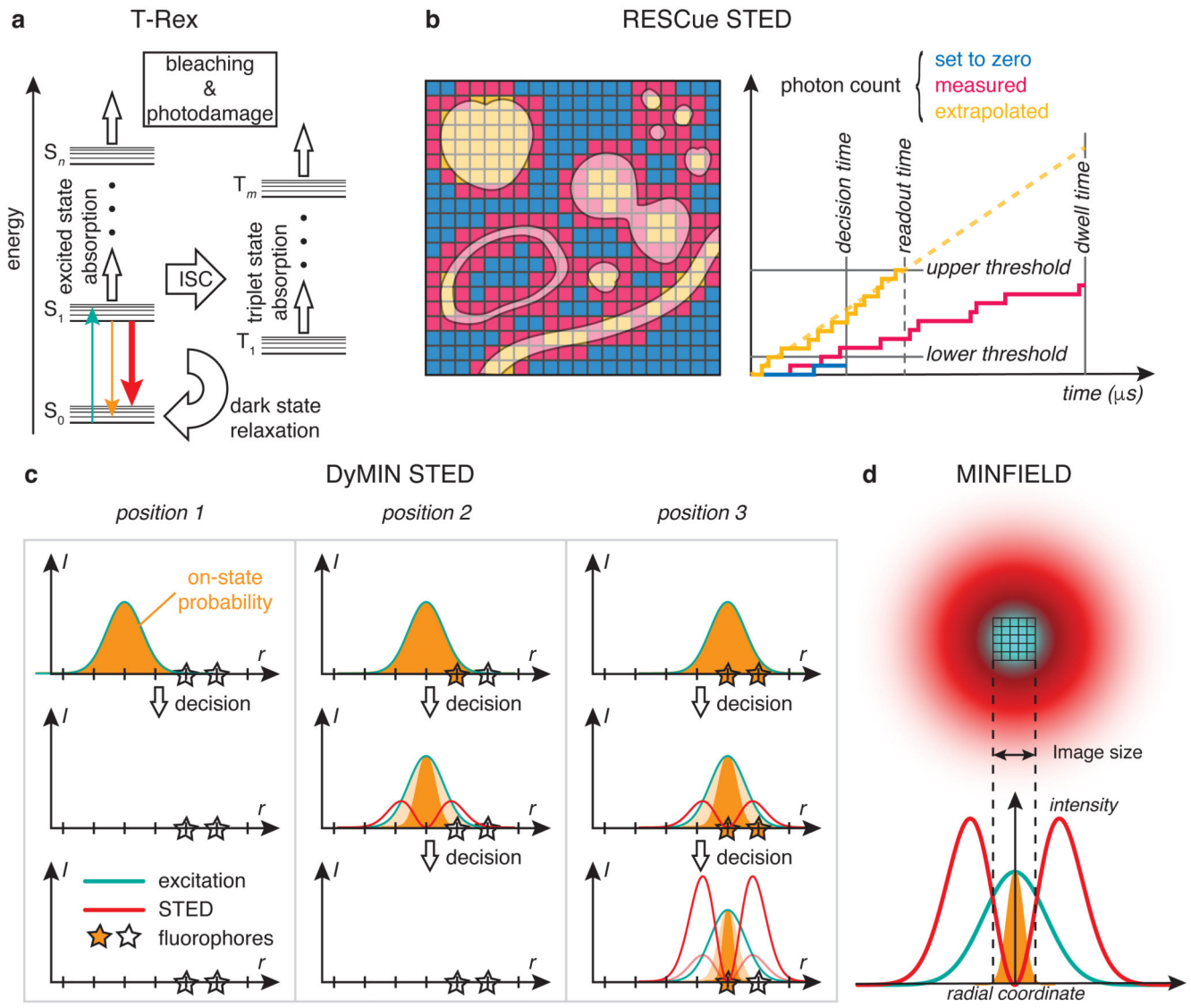

Figure 3.

Strategies to reduce light exposure and photobleaching in STED nanoscopy. a Dark/triplet state relaxation (T-Rex). Energy schematic for the relevant molecular states in STED microscopy. Fluorophores normally cycle between the ground state S_0 and the first excited state S_1 (same colour code for transitions as in Fig. 1). Excited state absorption drives fluorophores to higher lying molecular states S_n. Fluorophores undergoing intersystem crossing (ISC) to the triplet manifold may also absorb excitation and/or STED light and are particularly prone to chemical reactions, including radical generation. Residence times in triplet states are long (μs) compared to lifetimes of singlet excited states (ns). Dark (or triplet) state relaxation allows fluorophores to relax back to the singlet manifold. **b** RESCue STED. *Left:* Sample structure (shaded areas) with colour code for light exposure at each scan position (pixel). *Right:* Three exemplary photon counts as a function of time at different pixels. Blue: lower threshold is not reached at the decision time. Excitation and STED beams are turned off. Yellow: enough photons are collected to extrapolate from the readout

time to the full pixel dwell time with the desired signal-to-noise ratio. Lasers are turned off. Pink: the full pixel dwell time is used for collecting the signal. **c** DyMIN STED. Three exemplary light exposure sequences (top to bottom) at individual pixels. *Position 1:* No signal is collected in diffraction-limited mode. Lasers are turned off. *Position 2:* Signal is present in diffraction-limited mode. STED is turned on at the first power level. Since no more signal is present, a further increase in STED power would not yield additional information. *Position 3:* STED power is successively stepped up to the maximum value to separate fluorophores. Stars: fluorophores. Dark orange: normalized on-state probability defining resolution; light orange: resolution in previous intensity step; *r*, scan position; *I*, intensity. **d** In MINFIELD STED, the field of view is restricted to a region smaller than the extent of the doughnut beam, such that the region of interest is spared from exposure to the STED-light intensity maxima.

Europe PMC Funders Author Manuscripts

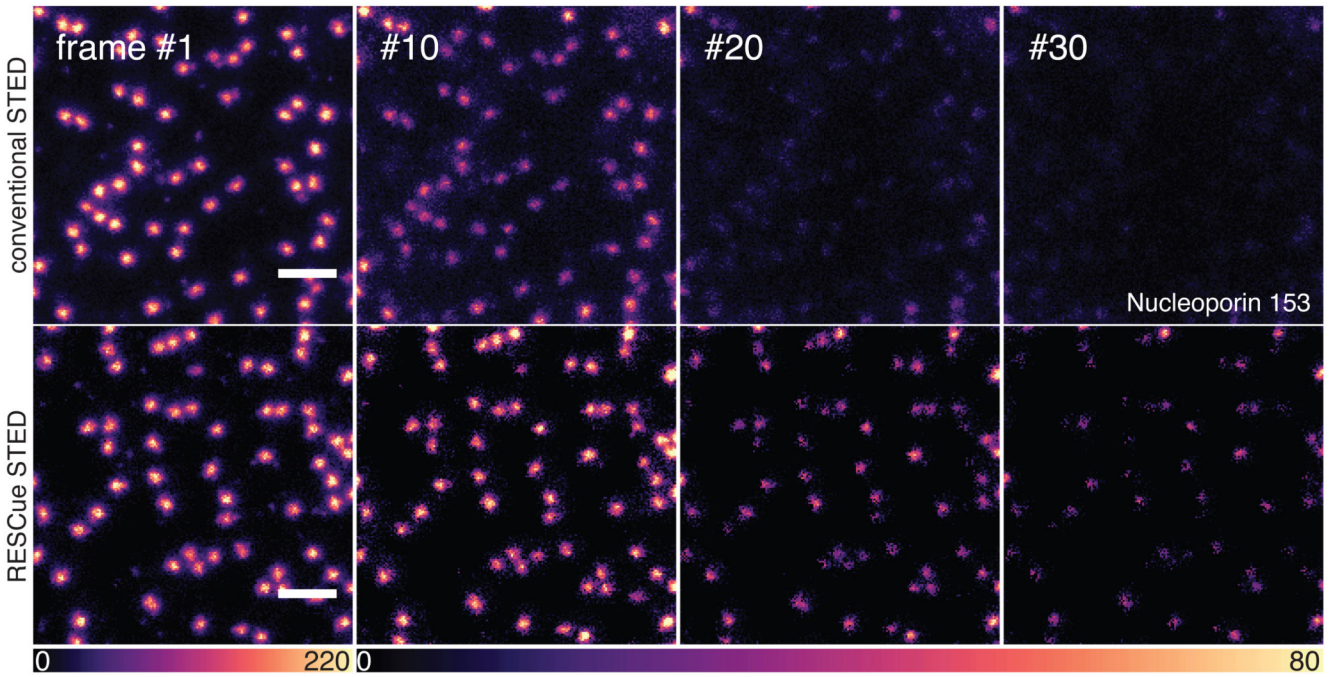

Figure 4.

RESCue STED attenuates photobleaching compared to conventional STED. Two regions of the same nucleus of a fixed U-2 OS cell immunostained for the nuclear pore protein Nucleoporin 153 with Abberior Star Red were each imaged 30 times using conventional STED (upper sequence) or RESCue STED (lower sequence). In an initial confocal probing step of 5 μs duration, a decision level of 30 photon counts was used to determine whether STED mode should be used at the respective pixel. For RESCue STED, four decision times with corresponding lower thresholds (lTh) were used for early laser shutdown: 1 count after 14% of the pixel dwell time, 3 counts after 24%, 6 counts after 37% and 16 counts after 79%. Upper threshold (uTh) that triggered premature laser shutoff and signal extrapolation was 50 counts. Pixel size was set to 15 nm with a dwell time of 40 μs, laser power at the sample was 1.7 μW for 640 nm excitation and 103 mW for 775 nm STED in both conditions. Scale bars: 500 nm. Note that the colour lookup table is different for frame #1 vs. the later frames.

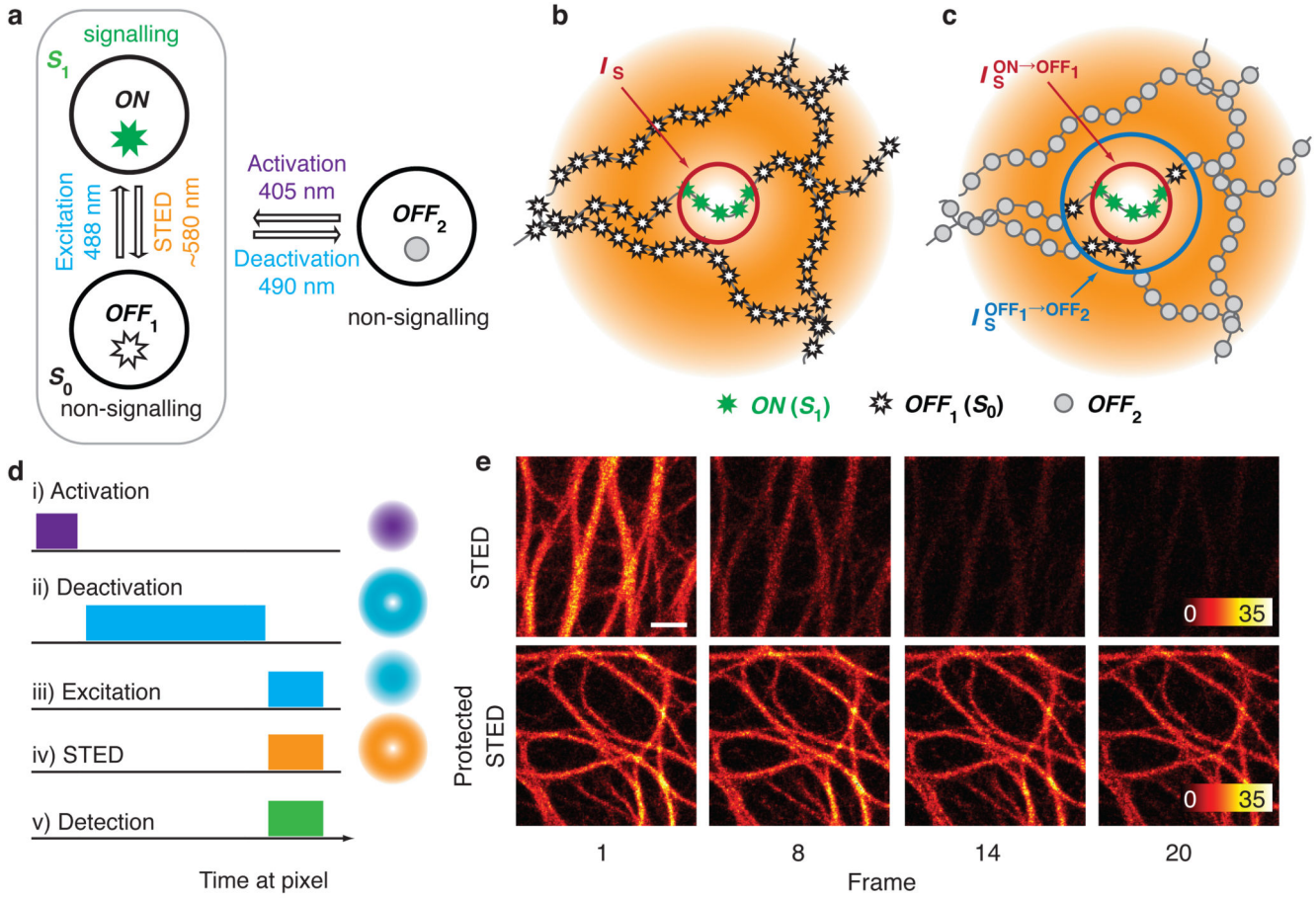

Figure 5.

Multiple off-state transitions for nanoscopy: protected STED. a Molecular state diagram for super-resolution imaging with multiple off-state transitions (MOST): In STED microscopy, a single off-transition is utilized to create the state contrast (grey box). In MOST nanoscopy, an additional off-state OFF_2 protects fluorophores and enhances state contrast. Wavelengths are exemplary for protected STED with rsEGFP variants. **b** In conventional STED, only fluorophores near intensity minima, where $I < I_S$, are allowed to fluoresce (green stars). In order to confine this region tightly, molecules away from the minimum (black stars) are exposed to high STED light intensities. **c** In protected STED mode, molecules are transferred to OFF_2 prior to subjecting them to STED (grey circles). $I_S^{OFF_1 \rightarrow OFF_2}$ is the intensity required to transfer molecules to OFF_2. **d** Sequence of light pulses and fluorescence detection at each scan position for protected STED imaging with corresponding light patterns in the focal plane. **e** Protected STED increases repeated imaging capability. Image series of living cells expressing keratin-rsEGFP2, imaged with conventional STED (top) and protected STED (bottom) with the same resolution and brightness in the first frame. Scale bar: 1 μm. Adapted from Danzl et al.[52].

Europe PMC Funders Author Manuscripts